NASA TECHNICAL NOTE

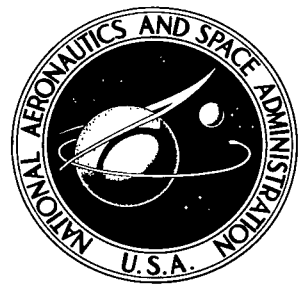

NASA TN D-8257

MINIMUM-MASS DESIGN OF FILAMENTARY COMPOSITE PANELS UNDER COMBINED LOADS: DESIGN PROCEDURE BASED ON SIMPLIFIED BUCKLING EQUATIONS

W. Jefferson Stroud and Nancy Agranoff

Langley Research Center
Hampton, Va. 23665

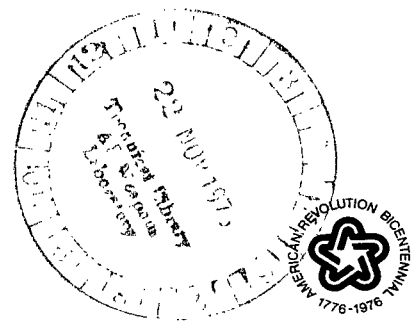

NATIONAL AERONAUTICS AND SPACE ADMINISTRATION • WASHINGTON, D. C. • OCTOBER 1976

1. Report No. NASA TN D-8257	2. Government Accession No.	3. Recipient's Catalog No.
4. Title and Subtitle MINIMUM-MASS DESIGN OF FILAMENTARY COMPOSITE PANELS UNDER COMBINED LOADS: DESIGN PROCEDURE BASED ON SIMPLIFIED BUCKLING EQUATIONS		5. Report Date October 1976 6. Performing Organization Code
7. Author(s) W. Jefferson Stroud and Nancy Agranoff		8. Performing Organization Report No. L-10770
9. Performing Organization Name and Address NASA Langley Research Center Hampton, VA 23665		10. Work Unit No. 505-02-42-01 11. Contract or Grant No.
12. Sponsoring Agency Name and Address National Aeronautics and Space Administration Washington, DC 20546		13. Type of Report and Period Covered Technical Note 14. Sponsoring Agency Code
15. Supplementary Notes		

16. Abstract

An analytical procedure is presented for designing hat-stiffened and corrugated panels made of composite material and subjected to longitudinal (in the direction of the stiffeners) compression and shear loadings. The procedure is based on nonlinear mathematical programing techniques and a simplified set of buckling equations. Design requirements considered are buckling, strength, and extensional and shear stiffness. Studies show the effects of specified thickness, variation of cross-section dimensions, stiffness requirements, local-buckling boundary conditions, and the effect of combined compression and shear loadings.

17. Key Words (Suggested by Author(s)) Stiffened panels Panel design Structural synthesis Structural design Minimum-mass design Composite panels Composite structure Structural efficiency	18. Distribution Statement Unclassified – Unlimited Subject Category 39	
19. Security Classif. (of this report) Unclassified	20. Security Classif. (of this page) Unclassified	21. No. of Pages 51 22. Price* $4.25

*For sale by the National Technical Information Service, Springfield, Virginia 22161

CONTENTS

MINIMUM-MASS DESIGN OF FILAMENTARY COMPOSITE PANELS UNDER COMBINED LOADS: DESIGN PROCEDURE BASED ON SIMPLIFIED BUCKLING EQUATIONS

W. Jefferson Stroud and Nancy Agranoff
Langley Research Center

SUMMARY

An analytical procedure is presented for designing hat-stiffened and corrugated panels made of composite material and subjected to longitudinal (in the direction of the stiffeners) compression and shear loadings. The procedure is based on nonlinear mathematical programing techniques and a simplified set of buckling equations. Design requirements considered are buckling, strength, and extensional and shear stiffness. Studies show the effects of specified thickness, variation of cross-section dimensions, stiffness requirements, local-buckling boundary conditions, and the effect of combined compression and shear loadings.

INTRODUCTION

Because composite materials offer the potential for substantial mass and cost savings, Langley Research Center is engaged in a broad program to study structural applications of filamentary composite materials. One objective of that program is to establish a mass and strength data base for generic structural components made of composite material. Such a data base, containing both analytical and experimental results, is necessary to develop confidence in composite structural design procedures. The generic component considered in this report is the stiffened panel: specifically, hat-stiffened and corrugated panels.

Some of the previous work dealing with the analysis and design of stiffened composite panels is discussed in references 1 to 6. The present report presents an analytical procedure for designing low-mass, hat-stiffened and corrugated panels which are subjected to longitudinal compression and shear loadings. Design studies carried out with the procedure are also presented.

The procedure is based on nonlinear mathematical programing techniques in which buckling, strength, and stiffness requirements as well as upper and lower bounds on cross-section dimensions are taken into account with inequality constraints. The objective is to

obtain minimum-mass designs. Overall-buckling loads are calculated by assuming smeared stiffnesses. Local-buckling loads are calculated by assuming simple-support boundary conditions along the lines of attachment of adjacent elements. Certain buckling modes (stiffener rolling, for example) are neglected in the buckling analyses used herein. Lamina stresses and strains are used in the strength calculations.

In composite-panel designs, the interaction of design variables may be quite complex. To demonstrate typical design study options available with the procedure presented in this report, studies were performed on hat-stiffened and corrugated graphite-epoxy panels loaded in compression and shear. These studies show the effects of discrete thickness, variations of cross-section dimensions, stiffness requirements, local-buckling boundary conditions, and the effect of combined compression and shear loadings. Detailed study results are presented so that a designer may obtain a better understanding of the mass penalties associated with practical design constraints such as stiffener cap widths and stiffener spacing.

SYMBOLS

Values are given in both SI and U.S. Customary Units. The calculations were made in U.S. Customary Units.

A	surface area of panel, pL
$\bar{A}$	area enclosed by hat (See eq. (A25).)
A_{ij}	laminate stiffnesses defined in equations (A1) and (A2)
A_{ij_k}	value of A_{ij} for element k
a	panel width (See fig. 5.)
b_k	element lengths defined in figure 2
D	depth of element 2 defined in figure 23
D_{ij}	laminate stiffnesses defined in equations (A1) and (A3)
D_{ij_k}	value of D_{ij} for element k

$D_1, D_2, D_3, D_x, D_y, D_{xy}$ — smeared orthotropic stiffnesses defined in equations (A10) to (A13)

d — distance between stiffeners; $2b_4$

E — Young's modulus

EI — beam bending stiffness of one period of panel cross section; defined in equation (A19)

ET — longitudinal extensional stiffness of panel; defined in equation (A5)

ET_k — longitudinal extensional stiffness for element k, defined in equation (A4)

E_1, E_2 — Young's modulus of composite material in fiber direction and transverse to fiber direction, respectively

G — shear modulus

GT — shear stiffness of panel; defined in equation (A6)

G_{12} — shear stiffness of composite material in coordinate system defined by fiber direction

L — panel length

N_x — applied longitudinal compressive loading per unit width of panel (See fig. 1.)

$N_{x,crit}$ — value of compressive load that causes buckling

N_{x_k} — longitudinal compressive loading in element k (See fig. 6.)

N_{xy} — applied shear loading per unit width of panel (See fig. 1.)

$N_{xy,crit}$ — value of shear load that causes buckling

N_{xy_k} — shear loading in element k (See fig. 6.)

N_y — applied transverse (y-direction) loading per unit width of panel

p	period of stiffened panel; $b_1 + 2b_4$
$Q_{11}, Q_{12}, Q_{22}, Q_{66}$	lamina stiffnesses
$t_k(\theta)$	thickness of lamina in element k at fiber orientation angle θ (See fig. 2.)
W	mass of one period of stiffened panel
$\frac{W/A}{L}$	mass index
w	lateral deflection of panel
x,y	coordinate directions; axes defined in figure 1
$\bar{z}$	vertical distance from neutral axis of element 3 to neutral axis of panel cross section
z_k	vertical distance from neutral axis of element 3 to neutral axis of element k
α	angle element 2 makes with the horizontal (See fig. 23.)
β	shear buckling parameter
$\bar{\gamma}_{xy}$	average overall shear strain of panel, defined by equation (A7)
$\epsilon_x, \epsilon_y, \gamma_{xy}$	laminate strains in X-Y coordinate system
$\epsilon_{y_k}, \gamma_{xy_k}$	laminate strains for element k
$\epsilon_1, \epsilon_2, \gamma_{12}$	lamina strains in coordinate system defined by fiber direction
θ	shear buckling parameter defined in equations (20) and (25), and fiber orientation angle shown in figure 1
μ	Poisson's ratio
μ_x, μ_y	Poisson's ratios associated with bending; defined by equation (A10)

μ_{12},μ_{21} Poisson's ratios of composite material in coordinate system defined by fiber direction

ρ density

$\sigma_1,\sigma_2,\tau_{12}$ lamina stresses in coordinate system defined by fiber direction

τ shear stress

Superscript:

a allowable

Subscript:

k integer denoting element number

LOADINGS AND CONFIGURATIONS CONSIDERED

Loadings

Two loadings are considered: a uniform, longitudinal compressive loading N_x in the direction of the stiffeners and a uniform shear loading N_{xy}. These loadings are shown in figure 1.

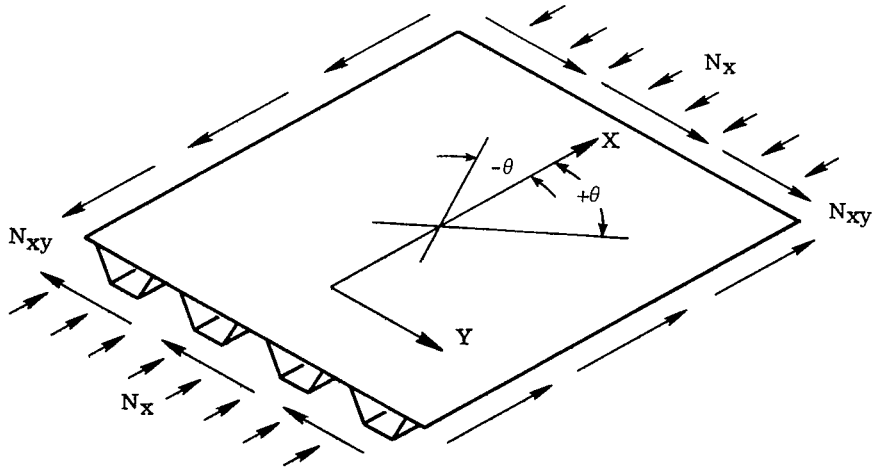

Figure 1.- Loadings considered.

Configurations

The two panel cross-sectional configurations considered in this report are shown in figure 2. The cross-section geometry is defined in terms of the four dimensions b_1, b_2, b_3, and b_4. The quantities b_1, b_2, and b_3 are the widths of elements 1, 2, and 3, respectively. The quantity b_4 is the half-width of element 4. Because of symmetry, b_4 is replaced by $\frac{b_3}{2}$ in the corrugated panel.

The panels are assumed to be made of a filamentary composite material with ply orientation angle θ measured from a line drawn in the direction of the stiffeners (the x-direction) as shown in figure 1. In the examples presented in this report, only two fiber orientations are considered: $\theta = 0^o$ and $\theta = \pm 45^o$. The 45^o plys are assumed to be balanced and symmetric and are, therefore, denoted $\pm 45^o$.

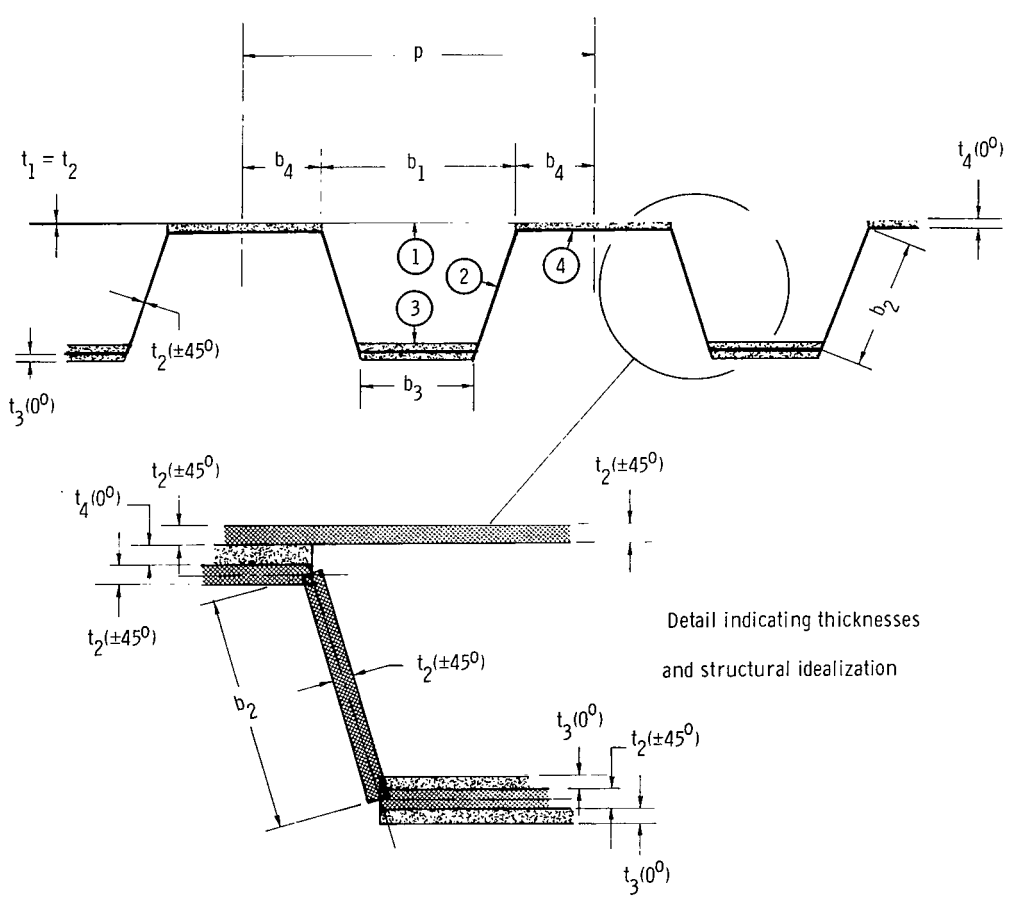

(a) Hat-stiffened panel.

Figure 2.- Configurations and design variables. Element identification numbers are indicated in figure 2(a).

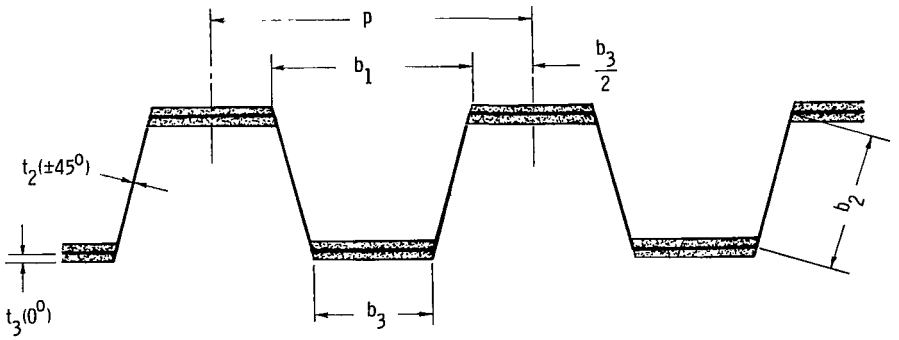

(b) Corrugated panel.

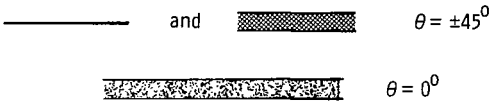

(c) Filament orientation pattern.

Figure 2.- Concluded.

All elements contain $\pm 45^0$ material. Elements 3 and 4 can also contain 0^0 material. The configurations are defined so that the 0^0 material and the $\pm 45^0$ material have specific locations. In both configurations $t_3(0^0)$ refers to the thickness of one of the two equal 0^0 layers in element 3; $t_4(0^0)$ is the thickness of a 0^0 layer sandwiched between $\pm 45^0$ skins in element 4.

The hat-stiffened configuration is a uniformly thick corrugated sheet of $\pm 45^0$ material attached to an equally thick flat sheet of $\pm 45^0$ material with 0^0 material at specified locations in elements 3 and 4. The corrugated configuration is a uniformly thick corrugated sheet of $\pm 45^0$ material with 0^0 material at specified locations in element 3. In both configurations, the thickness of a $\pm 45^0$ sheet is denoted $t_2(\pm 45^0)$ or simply t_2. The thicknesses of the $\pm 45^0$ sheets are taken to be uniform to provide a design that is relatively easy to fabricate.

ANALYSIS-DESIGN PROCEDURE

Nonlinear mathematical programing techniques are used to adjust the element widths and thicknesses (design variables) to provide minimum-mass designs that meet the design requirements. The design requirements (constraints) considered are strength, buckling, stiffness, and upper and lower bounds on the cross-section dimensions. The objective of

this section is to present and discuss briefly many of the expressions needed to evaluate the strength and buckling constraints. Equations for the extensional and shear stiffnesses are given in the appendix together with detailed expressions for other quantities that are used in this report.

Stress Analysis

The longitudinal and transverse strains and the longitudinal stress resultants are calculated for an applied longitudinal compressive load N_x. The transverse loading N_y is assumed to be zero for the overall panel and for each element that makes up the panel. The shear-stress resultants and shear strains are then calculated for an applied shear loading N_{xy}. Finally, by use of coordinate-transformation and stress-strain relations, the strains and stresses are calculated in the directions parallel and perpendicular to the fiber direction in each lamina of each element. All elements are assumed to be specially orthotropic (ref. 7) so that the inplane problem in each element is given by equation (A2) in the appendix.

The stress analysis equations are summarized in table I and are discussed in the text.

Longitudinal compression.- All elements of the panel cross section are assumed to have the same longitudinal strain ϵ_x given by equation (1). An expression for the longitudinal extensional stiffness ET of the panel cross section is given in the appendix. Since the transverse loading is assumed to be zero, the transverse strain ϵ_{y_k} in the kth element is given by equation (2). The longitudinal loading N_{x_k} in the kth element is proportional to the longitudinal extensional stiffness ET_k of that element and is given by equation (3).

Shear.- In the case of a hat-stiffened panel, the applied shear-stress resultant N_{xy} is assumed to be distributed over the panel cross section in the following manner. Element 4 carries the entire applied shear stress. In the region of the hat stiffener, the applied shear stress divides into two parts. Element 1 carries one part of the load, and elements 2 and 3 carry the other part. The relative proportions into which N_{xy} divides are obtained by equating the shear displacement of element 1 to the sum of the shear displacements of elements 2 and 3 as shown in figure 3. The resulting internal shear-stress resultants are given by equations (4) to (6), and the corresponding shear strains are given by equation (7). For a corrugated panel, the stiffness A_{66_1} is zero and $N_{xy_2} = N_{xy_3} = N_{xy}$.

During the synthesis, the internal stress resultants N_{x_k} and N_{xy_k}, given by equations (3) to (6), are compared with the local-buckling stress resultants discussed in a subsequent section.

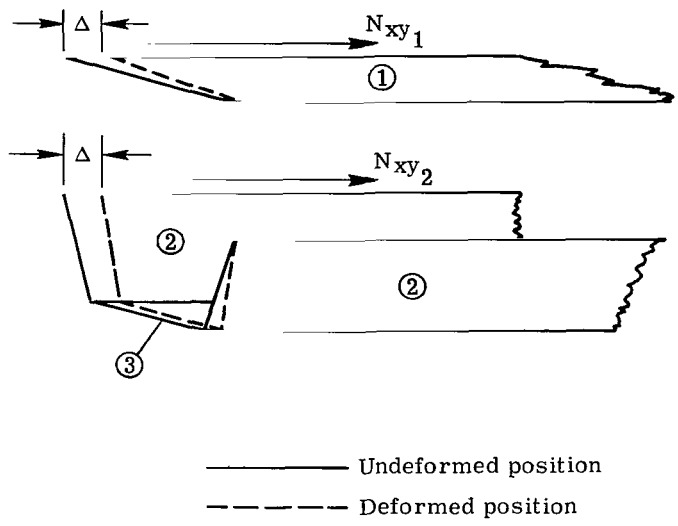

Figure 3.- Equating shear displacement of element 1 with sum of shear displacements of elements 2 and 3 to obtain internal shear-stress distribution.

Stresses and strains in each lamina.- With θ defined as the angle between the fiber direction and the x-direction (fig. 1), the strains in each lamina in the 1-direction, which is parallel to the fiber direction, and in the 2-direction, which is perpendicular to the fiber direction, are given by equations (8) to (10). The corresponding stresses in each lamina are given by equations (11) to (13).

The stresses and strains given by equations (8) to (13) are used in the strength criteria discussed in the next section. Since each element contains fibers oriented in both the $-\theta$ and $+\theta$ directions, stresses and strains at both orientations should be examined for strength considerations if shear loads exist.

Strength Failure Criteria

Several strength criteria have been proposed for designing filamentary composite laminates. Two criteria, referred to here as the maximum-strain criterion and the interactive-stress criterion, were used in the studies included in this report. (In no case were both criteria used simultaneously.) Both approaches appear, for example, in reference 8. The chosen failure criterion is applied to each lamina in each element.

The strength failure criteria equations are summarized in table II and are discussed in the text.

Maximum strain.- In the maximum-strain criterion, upper and lower limits are placed on the permissible values of ϵ_1, ϵ_2, and γ_{12}. The upper limit is used with

positive strains, and the lower limit with negative strains. In terms of inequality expressions, the maximum-strain criterion is given by equations (14) to (16) in which the superscript a means allowable, and signs and values of allowable strains must be selected to limit both positive and negative strains.

Stress interaction. - While each separate strain component is limited in the maximum-strain criterion, two of the stress components are linked in the stress-interaction criterion given here. Fiber failure is assumed to be prevented by equation (17), and matrix failure is assumed to be prevented by equation (18). Again, the superscript a means allowable, and signs and values of allowable stresses must be selected to limit both positive and negative stresses.

Buckling Analysis

The approach taken here is a traditional one in which buckling is assumed to be prevented if several independent forms of buckling, including overall- and local-buckling modes, are postulated and prevented. Overall-buckling equations are based on smeared stiffnesses, and local-buckling equations are based on simple-support boundary conditions along the lines of attachment of adjacent elements. (This same approach was used, for example, in refs. 9 and 10 and more recently in ref. 3.) This approach ignores compatibility of buckling mode shape, a factor that tends to make the approach conservative. On the other hand, the simplified analyses do not consider all the potential buckling modes, a factor that could make the approach unconservative. Unpublished studies with a more accurate buckling analysis indicate that in most cases the approach is sufficiently accurate to predict structural efficiencies and design trends. In some cases, such as those in which roll modes are active, the buckling analysis approach used here is not adequate.

Both the overall- and local-buckling analyses assume that the plate structure is orthotropic with principal axes alined with the edges of the plate. Buckling caused by longitudinal compression and buckling caused by shear are treated separately. Combined loads are accounted for with a buckling-interaction formula.

The buckling equations, which are based on work presented in references 8 and 11 to 15, are summarized in table III and are discussed in the text. Certain detailed expressions, including equations for the smeared orthotropic stiffnesses, are presented in the appendix.

Overall buckling. - The order of presentation is longitudinal compression, shear, and combined longitudinal compression and shear.

Longitudinal compression: The stiffened panel is treated as a wide column with the loaded ends simply supported and with the lateral edges free as shown in figure 4. A

buckling equation that takes into account transverse shear effects is presented as equation (19) in table III. The transverse shearing-stiffness term is taken as $2 \cdot b_2 \cdot A_{66_2}$.

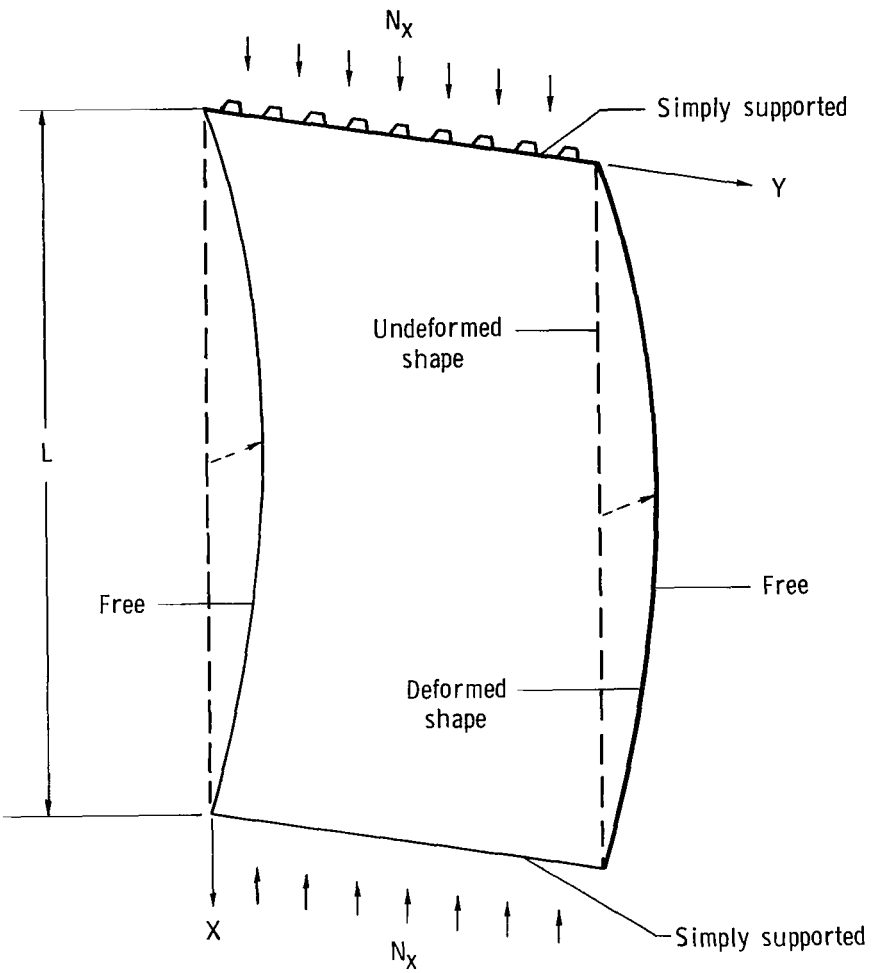

Figure 4.- Wide-column or Euler buckling is assumed for overall buckling in axial compression.

Shear: The panel is assumed to be long in the y-direction and simply supported along the edges $x = 0$ and $x = L$ as shown in figure 5. The buckling equations are given as equations (20) to (22) in table III.

Equations (21) and (22) are based on the assumption that the smeared bending stiffness in the x-direction D_1 is much larger than the smeared bending stiffness in the y-direction D_2, and on the assumption that the dimension a (fig. 5(a)) is larger than the dimension L. These assumptions permit a parameter β defined by

$$\beta = \frac{L}{a}\left(\frac{D_2}{D_1}\right)^{1/4}$$

to be taken as zero in the derivation of equations (21) and (22). The equations correspond, therefore, to the infinitely long panel shown in figure 5(b).

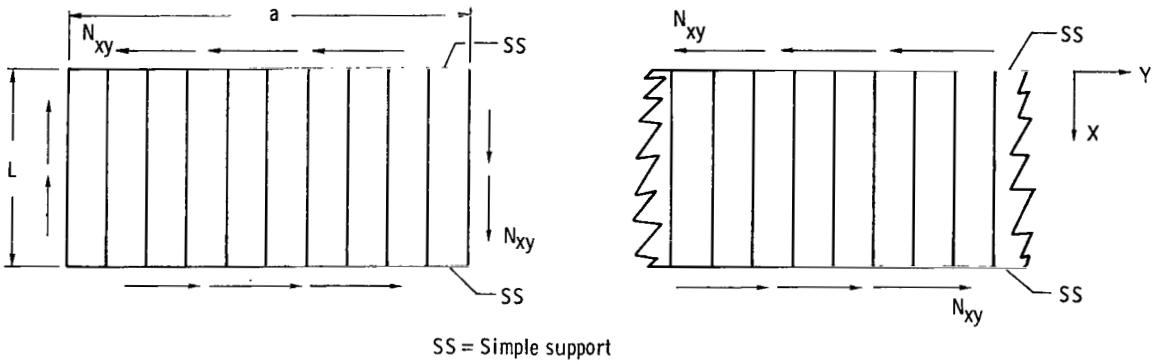

(a) Finite shear model. (b) Infinitely long shear model.

Figure 5.- Finite and infinitely long shear models for overall shear buckling.

Combined longitudinal compression and shear: When both longitudinal compression and shear loadings are present, buckling is assumed to occur when the buckling-interaction formula given by equation (23) is satisfied. Based on studies of isotropic plates in reference 14 and orthotropic plates in reference 15, this buckling-interaction formula appears to be adequate for the panels and loadings considered herein.

Local buckling.- The second level subscript (indicating the kth element) is dropped in table III and elsewhere in this report except where it is necessary for clarity.

Longitudinal compression: The structural model is shown in figure 6. The length L of each element is assumed to be much greater than its width b. With these simplifying assumptions the buckling equation, which is applied to each of the four elements of the cross section, is given by equation (24).

Shear: Local shear buckling is treated in the same way that overall shear buckling was treated in an earlier section. The only difference is the stiffnesses that are used. Again, the structural model is shown in figure 6. The equations for local shear buckling are given by equations (25) to (27) in table III.

Equations (26) and (27) are based on the assumption that $L >> b$ (fig. 6). This assumption permits a parameter β defined by

$$\beta = \frac{b}{L}\left(\frac{D_{11}}{D_{22}}\right)^{1/4}$$

to be taken as zero in the derivation of equations (26) and (27).

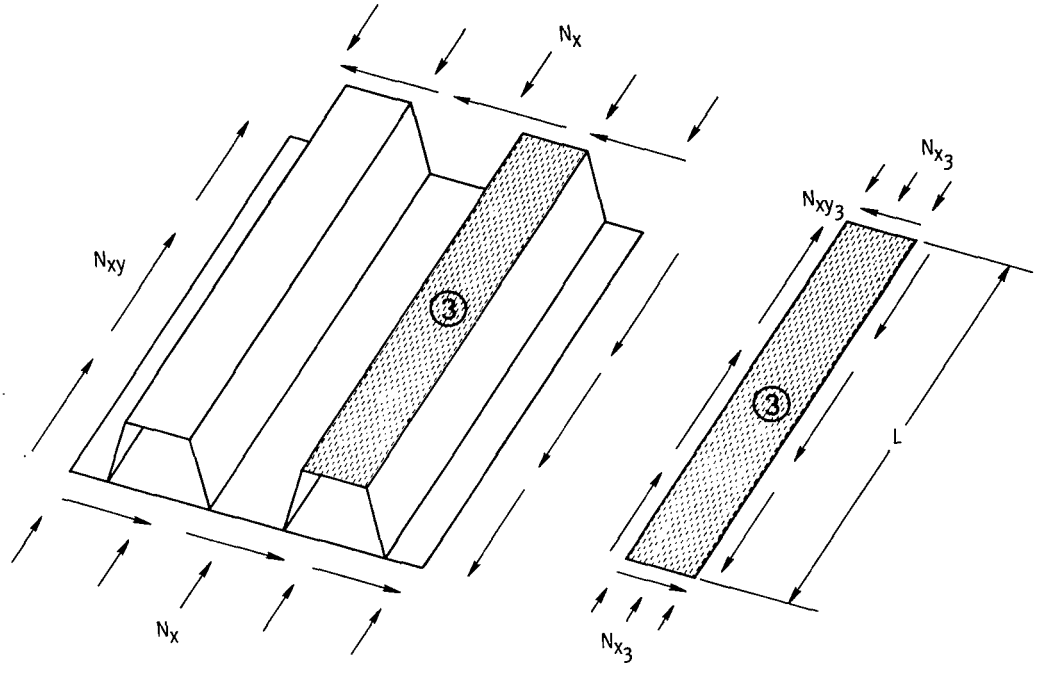

Figure 6.- Example of strip element used for local buckling.

Combined longitudinal compression and shear: The buckling-interaction formula given by equation (23) is used for local as well as overall buckling. The adequacy of that formula is examined and verified for orthotropic plates in reference 15.

Sizing Technique

The design problem is formulated as a nonlinear mathematical programing problem. The design variables are the element widths and thicknesses that define the cross section. The constraints are the strength, buckling, and stiffness design requirements. Since the panel length L is fixed, the objective function (the quantity that is minimized) is the panel mass per unit width. Equations for the strength and buckling constraints have been presented in the preceding sections. Equations for the stiffnesses are given in the appendix.

The specific design constraints considered herein are overall buckling, local buckling of each element, strength of each lamina in each element, extensional stiffness, and shear stiffness. Upper and lower bounds are also placed on various dimensions.

The computer program used to perform the optimization in the studies presented herein is a general-purpose parameter optimizer denoted AESOP (refs. 16 to 18) which accounts for constraints using an exterior penalty function approach. The AESOP code contains several optimization algorithms that can be selected in various combinations by the user. The approach used here was a combination called "creeper" and "pattern." These algorithms are described in references 16 to 18.

DESIGN STUDIES CARRIED OUT WITH ANALYSIS-DESIGN PROCEDURE

Studies were carried out to examine detailed design trends, sensitivity of structural efficiency to changes in certain dimensions, effect of extensional and shear-stiffness design requirements, effect of local buckling boundary conditions, and the effect of combined compression and shear loadings. The material properties that are used for all studies are given in tables IV and V. The upper and lower limits placed on the cross-section dimensions are given in table VI.

Structural Efficiency Diagrams and Scaling

The structural design data developed in this report are presented in the form of structural efficiency diagrams in which the mass index $\frac{W/A}{L}$ of minimum-mass panels is given as a function of the loading index $\left(\frac{N_x}{L} \text{ or } \frac{N_{xy}}{L}\right)$, also called the structural index. Presenting design data in this manner minimizes size effects and broadens the applicability of the data. If there were no upper or lower limits on the cross-sectional dimensions and if the thickness could vary continuously, then size effects would be eliminated. Size effects are eliminated because of dimensional similarity or scaling principles that apply to composite panels in the same way that they have been applied to conventional metal panels. (See, for example, ref. 19.)

The scaling principle for panels with loadings considered herein can be summarized as follows. If two panels have the same proportions – that is, if all the dimensions (including thicknesses and length) of one panel are multiplied by a single scale factor to obtain the dimensions of the other panel – and if both panels are subjected to loads which give the same value of the loading index, then

(1) the stresses in the corresponding laminas are the same for both panels;

(2) the ratios of the element stress resultants to the element buckling-stress resultants are the same for both panels;

(3) the ratio of the overall stress resultant to the overall buckling-stress resultant is the same for both panels; and

(4) the mass index is the same for both panels.

These four statements confirm that for a given structural concept (including the material system), minimum-mass designs fall on a single structural efficiency curve and that dimensions of minimum-mass panels scale linearly with the load (not the load index).

The results are presented in terms of dimensional quantities. In some cases, for example, t_2 is used as a parameter. In all cases the data are for panels with $L = 0.76$ m (30 in.). It is understood that scaling techniques can be applied to the results to make them applicable to other panel sizes and loads. For example, curves for which t_2 is constant can be interpreted as curves for which $\frac{t_2}{L}$ is constant.

Hat-Stiffened Panel, Longitudinal Compressive Loading N_x

Effect of discrete values of thickness $t_2(\pm 45^o)$. - Minimum values of the mass index $\frac{W/A}{L}$ are given in figure 7 as a function of compressive loading index $\frac{N_x}{L}$ for various values of $t_2(\pm 45^o)$. It is assumed that the thickness of 0^o material can vary continuously. The values chosen for t_2 represent four-ply and eight-ply laminates made up of plies of either 0.051 mm (0.0020 in.) or 0.140 mm (0.0055 in.) thickness. Laminates that are multiples of four plys can be made balanced and symmetric; balanced and symmetric laminates are required in all the studies presented in this report. The curves give an indication of the range over which a particular value of t_2 is lightest and the penalty involved in selecting another thickness.

The dashed curve indicates designs for which $t_2(\pm 45^o)$ is allowed to vary continuously. That curve is referred to as the $t_2$free curve. It is tangent to the various curves for which t_2 is constant. The designs associated with the $t_2$free curve are referred to as the $t_2$free designs.

The requirement that elements 1 and 3 have a width not less than 2.03 cm (0.80 in.) begins to have an effect for loadings less than $\frac{N_x}{L} = 276$ kPa (40 lbf/in^2) where the $t_2$free curve begins to deviate from a straight line.

All the examples presented herein use the interactive-stress criterion given by equations (17) and (18). For loadings greater than $\frac{N_x}{L} = 3.45$ MPa (500 lbf/in^2), strength considerations begin to affect the $t_2$free designs and the designs for which $t_2 = 1.12$ mm (0.044 in.). For this hat-stiffened configuration and for the material properties (table IV) used for these studies, the maximum strain requirement (eqs. (14) to (16)) produces slightly heavier designs than the interactive-stress requirement. For example, at $\frac{N_x}{L} = 6.89$ MPa (1000 lbf/in^2) where the difference is largest, the maximum strain designs

are about 4 percent heavier than the interactive-stress designs. This is the only study reported in this paper in which the maximum-strain criterion is used. Strength requirements do not affect the designs with the other values of t_2 shown in figure 7.

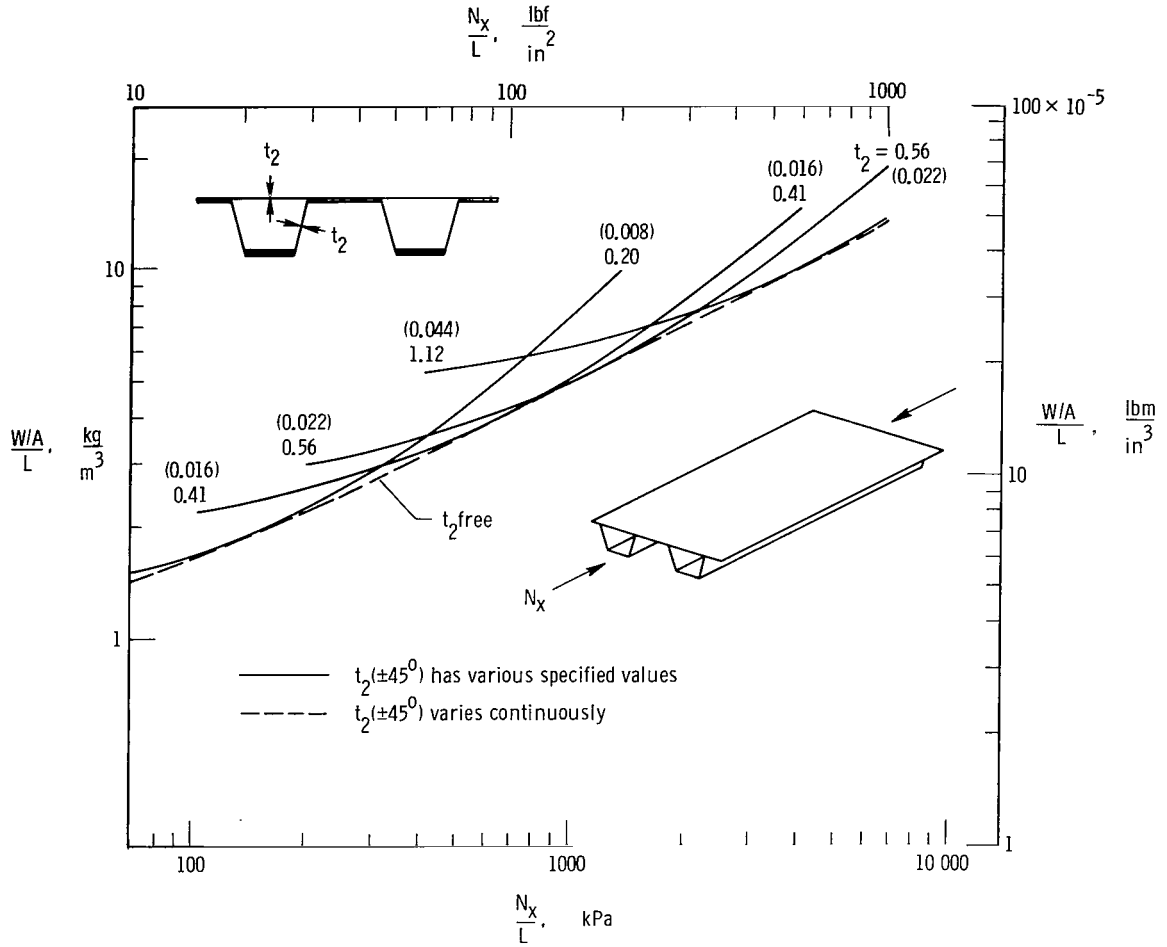

Figure 7.- Structural efficiency of graphite-epoxy, hat-stiffened compression panels for various prescribed values of thickness t_2 and for t_2 varying continuously; L = 0.76 m (30 in.); thickness t_2 is shown in mm (in.).

Consider the loading $\frac{N_x}{L}$ = 689 kPa (100 lbf/in^2). The lightest design has t_2 equal to about 0.41 mm (0.016 in.). Manufacturing requirements may, however, make it more desirable to fabricate a design with t_2 equal to 0.56 mm (0.022 in.). The cross sections for the minimum-mass designs having t_2 equal to 0.41 mm and 0.56 mm are presented in figure 8. The design for which t_2 = 0.56 mm is larger and deeper than the design for which t_2 = 0.41 mm. (Both designs are penalized slightly by the $b_3 \geq 2.03$ cm (0.80 in.) requirement.)

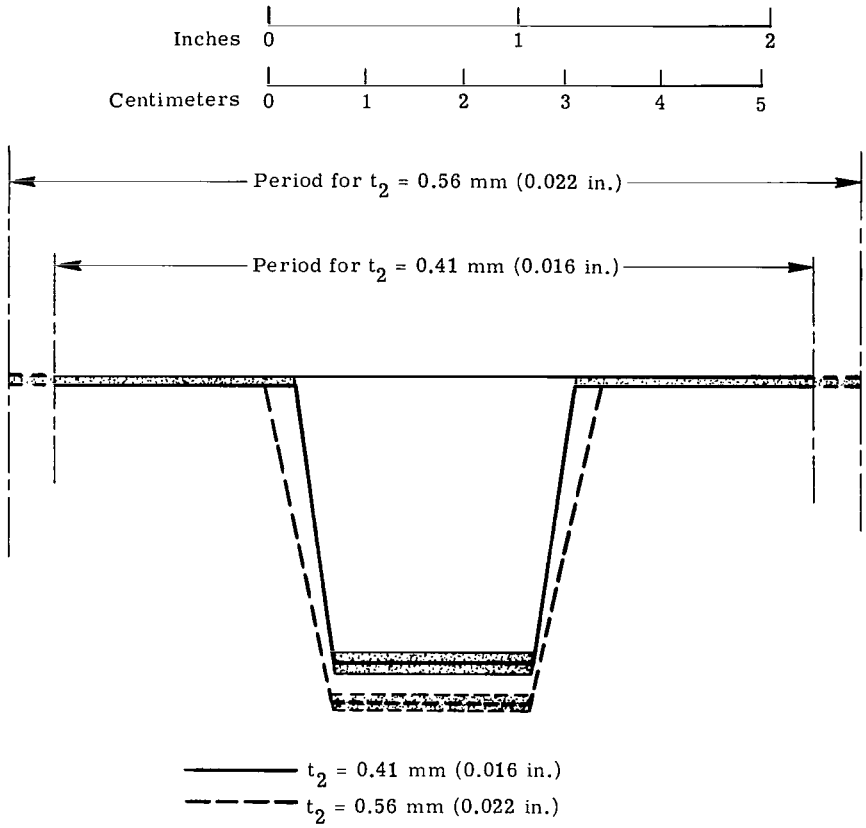

Figure 8.- Cross sections for two hat-stiffened panels designed for $\frac{N_x}{L}$ = 689 kPa (100 lbf/in^2); L = 0.76 m (30 in.).

The significant point here is that even though t_2 is increased from 0.41 mm (0.016 in.) to 0.56 mm (0.022 in.) – a 37-percent increase – the design for which t_2 = 0.56 mm is only 4-percent heavier than the design for which t_2 = 0.41 mm. In this case, as well as in many other cases, the manufacturing requirement on the thickness t_2 can be accommodated with very little penalty in structural efficiency. It should be pointed out, however, that although there is very little difference in the mass of the two designs, the extensional and the shearing stiffnesses of the one design differ substantially from the corresponding stiffnesses in the other design. This fact is discussed in more detail in a subsequent section.

Variation of dimensions as function of $\frac{N_x}{L}$ for t_2 = 0.56 mm (0.022 in.).- Cross-section dimensions of the designs in figure 7 for which t_2 = 0.56 mm (0.022 in.) are presented as a function of the loading index $\frac{N_x}{L}$ in figure 9. These dimensions are for

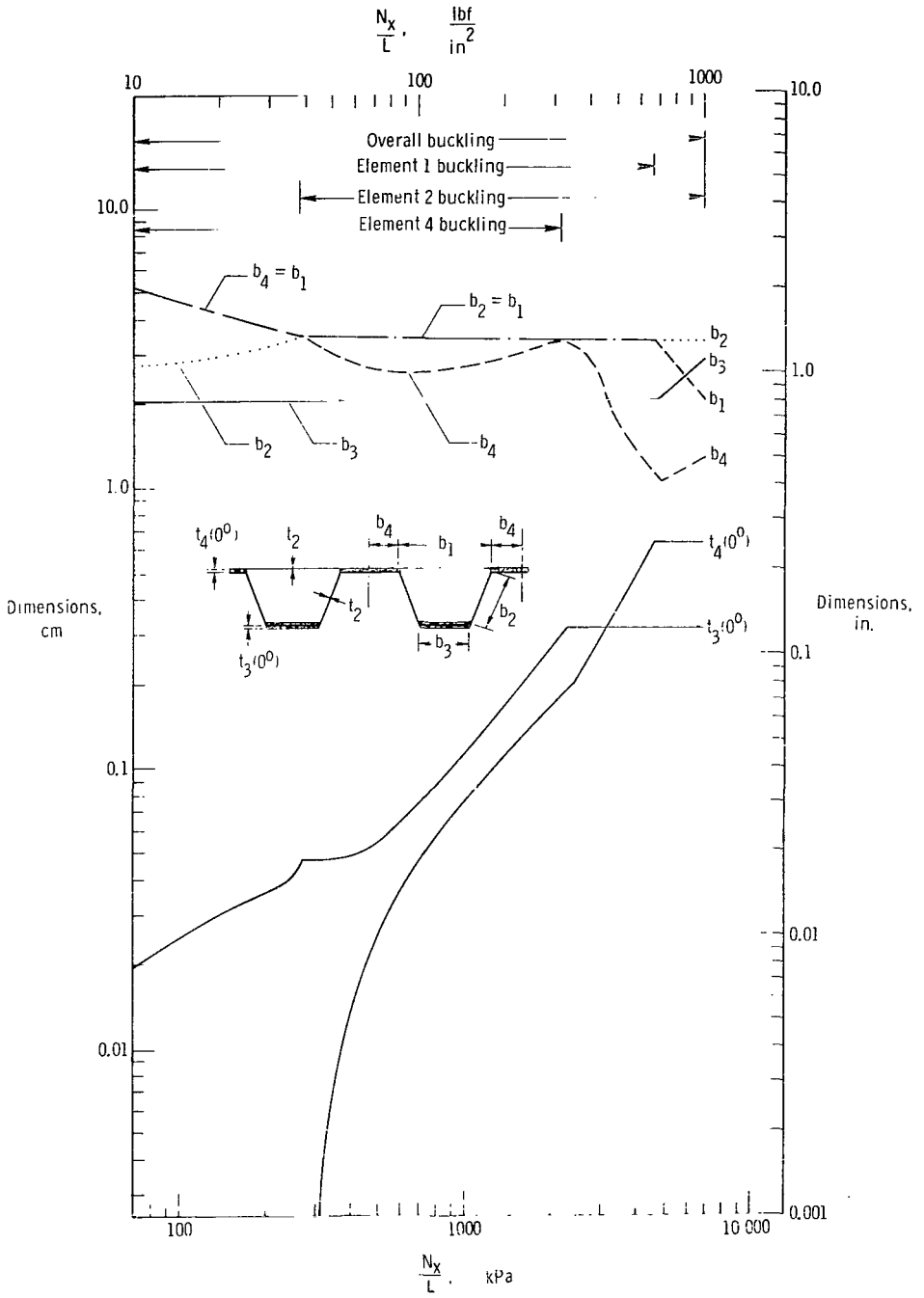

Figure 9.- Variation of cross-sectional dimensions as function of loading for minimum-mass, hat-stiffened, graphite-epoxy compression panels; t_2 = 0.56 mm (0.022 in.); L = 0.76 m (30 in.).

a panel with a length L of 0.762 m (30 in.) and for the material properties of table IV. The loading ranges over which various buckling constraints are active are given at the top of figure 9. Element 3 is not buckling critical over the loading range shown in figure 9.

The width b_3 of element 3 is shown in figure 9 as being equal to its minimum value (2.03 cm (0.80 in.)) until $\frac{N_x}{L}$ is equal to about 4830 kPa (700 lbf/in^2). Actually, b_3 has a weak tendency to increase to a larger value over the range $\frac{N_x}{L}$ = 2410 to 3450 kPa (350 to 500 lbf/in^2). This increase in b_3 is accompanied by a decrease in $t_3(0^o)$ so that at a given loading the total longitudinal extensional stiffness $(ET_3 \cdot b_3)$ of element 3 remains almost constant regardless of the relative values of b_3 and $t_3(0^o)$. The simple variation of b_3 and $t_3(0^o)$ is shown in figure 9 for clarity. The weak tendency of b_3 to exceed its minimum value in the above loading range is discussed in the next section.

Cross-section shapes of the panels having t_2 = 0.56 mm (0.022 in.) and designed to support loadings of $\frac{N_x}{L}$ = 68.9, 689, and 6890 kPa (10, 100, and 1000 lbf/in^2) are presented in figure 10. The designs for $\frac{N_x}{L}$ = 68.9 and 6890 kPa are shown merely to indicate the design trends for a fixed value of t_2. Other values of t_2 provide substantially lighter designs at these two loadings.

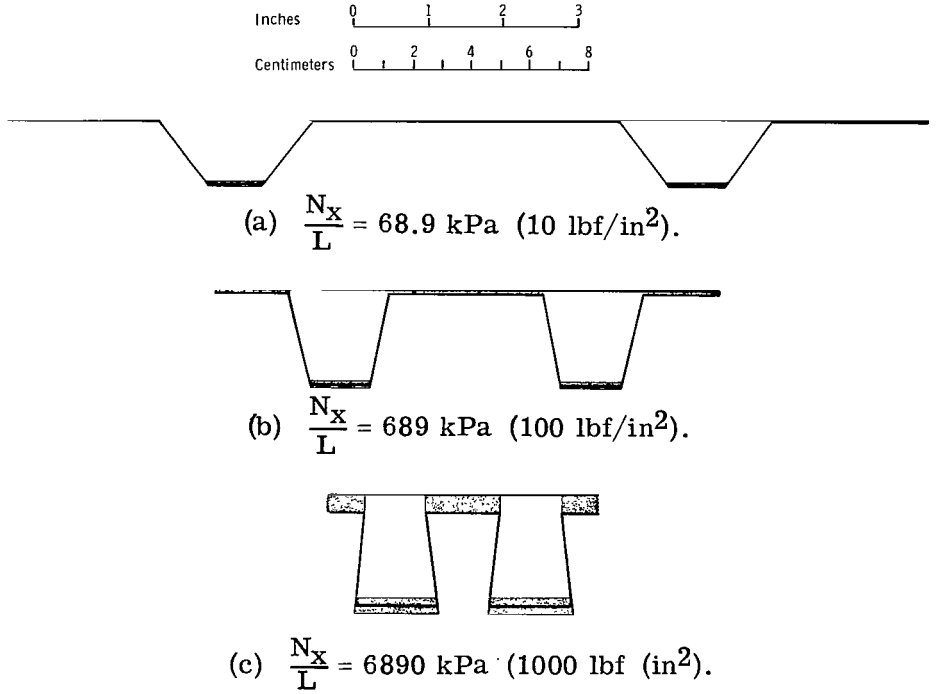

(a) $\frac{N_x}{L}$ = 68.9 kPa (10 lbf/in^2).

(b) $\frac{N_x}{L}$ = 689 kPa (100 lbf/in^2).

(c) $\frac{N_x}{L}$ = 6890 kPa (1000 lbf (in^2).

Figure 10.- Cross-sectional shapes of hat-stiffened, graphite-epoxy compression panels having t_2 = 0.56 mm (0.022 in.) and L = 0.76 m (30 in.) for three values of axial compressive load.

Effect of changes in width of element 3.- In the previous section it was pointed out that although the width b_3 of element 3 is shown in figure 9 as being equal to the minimum value (2.03 cm (0.80 in.)) until $\frac{N_x}{L}$ is equal to about 4830 kPa (700 lbf/in^2), there is actually a weak tendency for b_3 to be larger than the minimum value in the region $\frac{N_x}{L}$ = 2410 to 3450 kPa (350 to 500 lbf/in^2). That effect is shown in figure 11 for a loading of $\frac{N_x}{L}$ = 2760 kPa (400 lbf/in^2). In figure 11 stiffened panels are completely redesigned for various prescribed values of b_3; that is, each point shown by a circular symbol represents a minimum-mass design for that value of b_3. For these calculations, t_2 = 0.56 mm (0.022 in.). The minimum value of the mass index $\frac{W/A}{L}$ occurs at b_3 equal to about 2.54 cm (1.0 in.). For this loading, the penalty for choosing b_3 = 2.03 cm is about 0.25 percent. It is apparent that for this value of $\frac{N_x}{L}$, the width b_3 can vary over a large range with very little change in structural efficiency. The width b_3 is a weak design variable for other loadings also. This fact can be exploited to accommodate manufacturing or other design considerations.

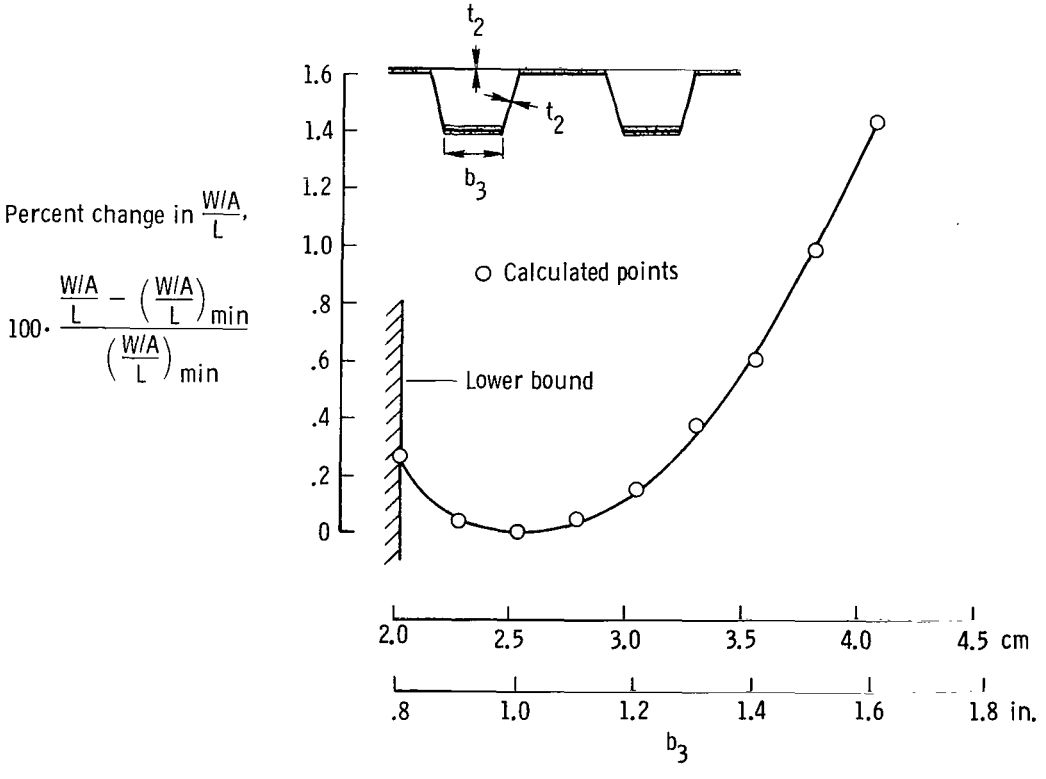

Figure 11.- Percent change in structural efficiency as function of dimension b_3 for minimum-mass, graphite-epoxy, hat-stiffened compression panels; t_2 = 0.56 mm (0.022 in.); L = 0.76 m (30 in.); $\frac{N_x}{L}$ = 2760 kPa (400 lbf/in^2).

Effect of changes in width of element 4.- The structural efficiency is more sensitive to changes in b_4 than to changes in b_3. An indication of that sensitivity is shown in figure 12 in which the percent change in mass index is presented as a function of width d (twice b_4) of the flat portion between stiffeners for two values of $\frac{N_x}{L}$: 689 and 4830 kPa (100 and 700 lbf/in^2). The circular and square symbols indicate minimum-mass designs for the 689 and 4830 kPa cases, respectively. For these results, the thickness t_2 is allowed to vary freely.

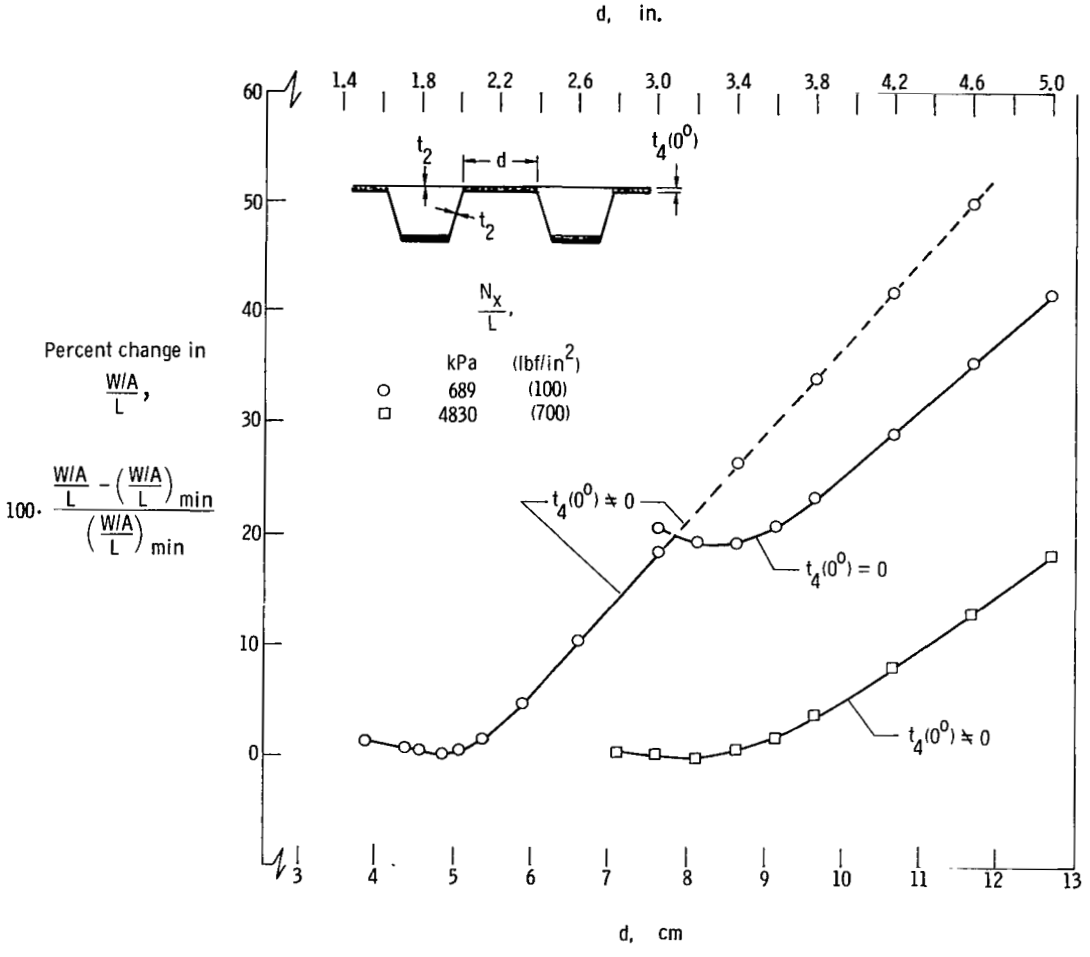

Figure 12.- Effect on structural efficiency of increasing stiffener spacing d of hat-stiffened, graphite-epoxy compression panels; t_2 varies continuously; L = 0.76 m (30 in.).

First, consider the case for which $\frac{N_x}{L}$ = 689 kPa (100 lbf/in^2). With no constraint placed on d, the lightest design occurs for d equal to about 4.8 cm (1.9 in.). As d

is increased, the mass index $\frac{W/A}{L}$ increases. When d is equal to about 7.9 cm (3.1 in.), the lightest design changes from one with 0^o material in elements 3 and 4 to one that has 0^o material in element 3 only $\left(t_4(0^o) = 0\right)$. The two concepts, one with and the other without 0^o material in element 4, do not evolve from one another. They are completely independent. The concept with no 0^o material in element 4 is similar to those for low loadings shown in figure 9 in that b_1 is equal to b_4. As d is increased from about 4.8 cm to 12.7 cm (5.0 in.), the mass index increases by about 42 percent.

For the case in which $\frac{N_x}{L}$ = 4830 kPa (700 lbf/in^2), the efficiency of the concept for which $t_4(0^o) = 0$ is restricted because of the upper bound placed on $t_3(0^o)$ and because of strength considerations. For these reasons, the concept with 0^o material in both elements 3 and 4 is lighter than the concept with 0^o material in only element 3 for the entire range of d considered. The lightest design occurs for d equal to about 8.1 cm (3.2 in.). As d is increased to 12.7 cm (5.0 in.), the mass index increases by about 18 percent.

Another way of studying the effect of increasing the distance d between stiffeners is with a structural efficiency diagram such as that shown in figure 13. The objective here is to show the effects of a constraint defined by $d \geqq 12.7$ cm (5.0 in.). Since there is no tendency for d to be greater than 12.7 cm for the cases considered, the constraint becomes simply d = 12.7 cm.

The bottom solid curve in figure 13 gives the structural efficiency of hat-stiffened designs with no constraint on d. It is the $t_2$free curve of figure 8. The two dashed curves that are tangent to the $t_2$free curve are portions of the corresponding curves of figure 8. Like the solid curve, these two dashed curves have no constraint on d and are used for reference. For the other curves, d is required to be 12.7 cm (5.0 in.).

The other solid curve in figure 13 forms the lower bound for the designs having d = 12.7 cm (5.0 in.). For this curve, t_2 is allowed to vary freely. For loadings less than about $\frac{N_x}{L}$ = 3450 kPa (500 lbf/in^2), the designs for which $t_4(0^o) = 0$ are lighter than the designs for which $t_4(0^o) \neq 0$. However, because of the upper bound on $t_3(0^o)$ and because of strength considerations, the designs for which $t_4(0^o) \neq 0$ are lighter for loadings greater than about $\frac{N_x}{L}$ = 3450 kPa (500 lbf/in^2).

The penalty in structural efficiency caused by increasing the distance d between stiffeners to 12.7 cm (5.0 in.) depends upon the loading level. At $\frac{N_x}{L}$ = 68.9 kPa (10 lbf/in^2), the increase in the mass index is about 77 percent; at $\frac{N_x}{L}$ = 6890 kPa (1000 lbf/in^2), the increase is about 14 percent.

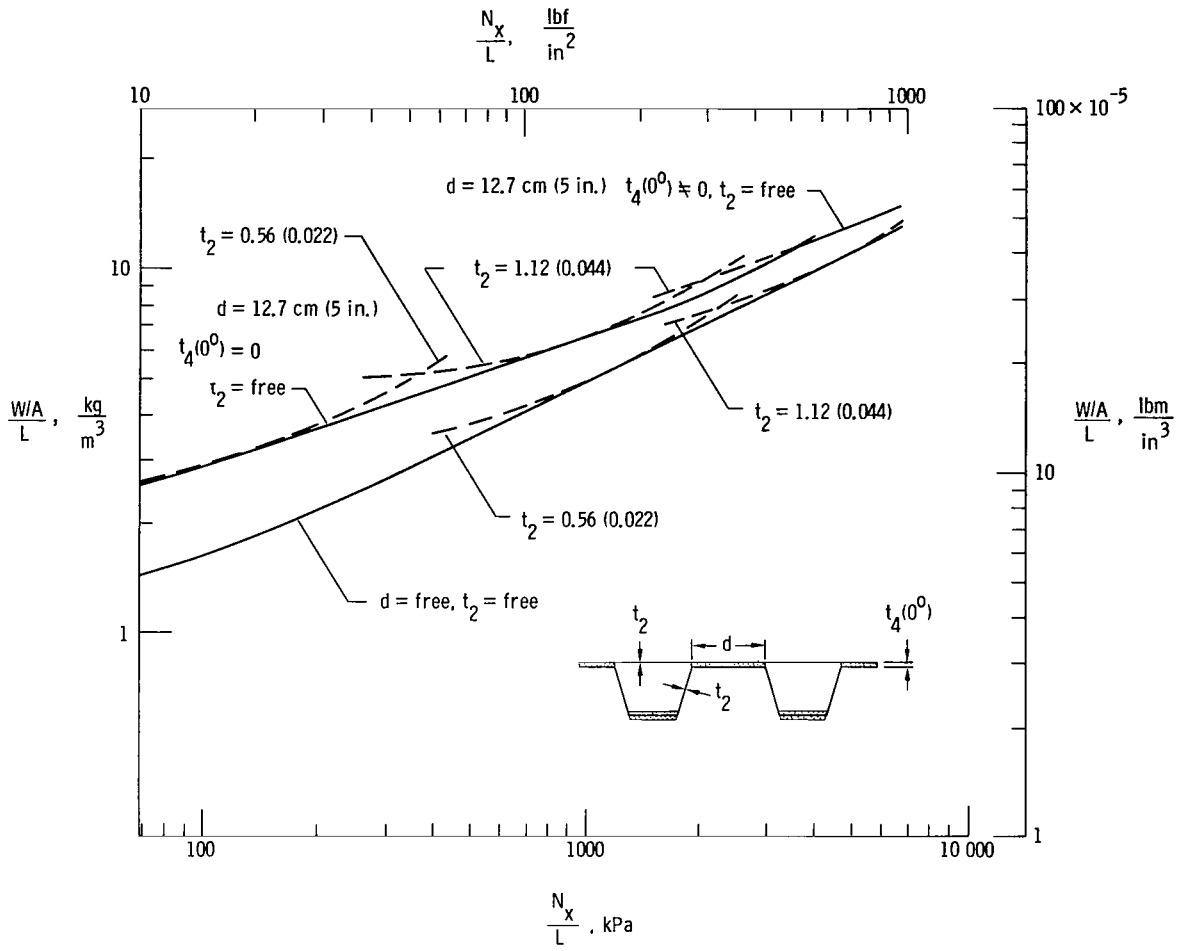

Figure 13.- Effect of d = 12.7 cm (5 in.) stiffener spacing requirement on structural efficiency of hat-stiffened, graphite-epoxy compression panels. Thicknesses are shown in mm (in.); L = 0.76 m (30 in.).

Effect of local-buckling boundary conditions.- As explained earlier, the analysis for local buckling is based on the assumption that each element is simply supported along its line of attachment to the adjacent elements. This assumption is believed to be conservative in most cases. In particular, since element 3 never experiences local buckling in the designs generated in this report, it is reasonable to assume that element 3 provides rotational support to element 2 and that a more sophisticated analysis-design procedure could exploit that extra support.

To assess the effect of local-buckling boundary conditions and to provide information on the potential benefits available with a more sophisticated analysis, additional designs were generated under the assumption that the local-buckling boundary conditions for

elements 1 and 2 were clamped rather than simply supported. The results are presented in figure 14. The solid curves represent designs obtained with the clamped boundary condition assumption, and the dashed curves are the original designs with the simple-support boundary conditions.

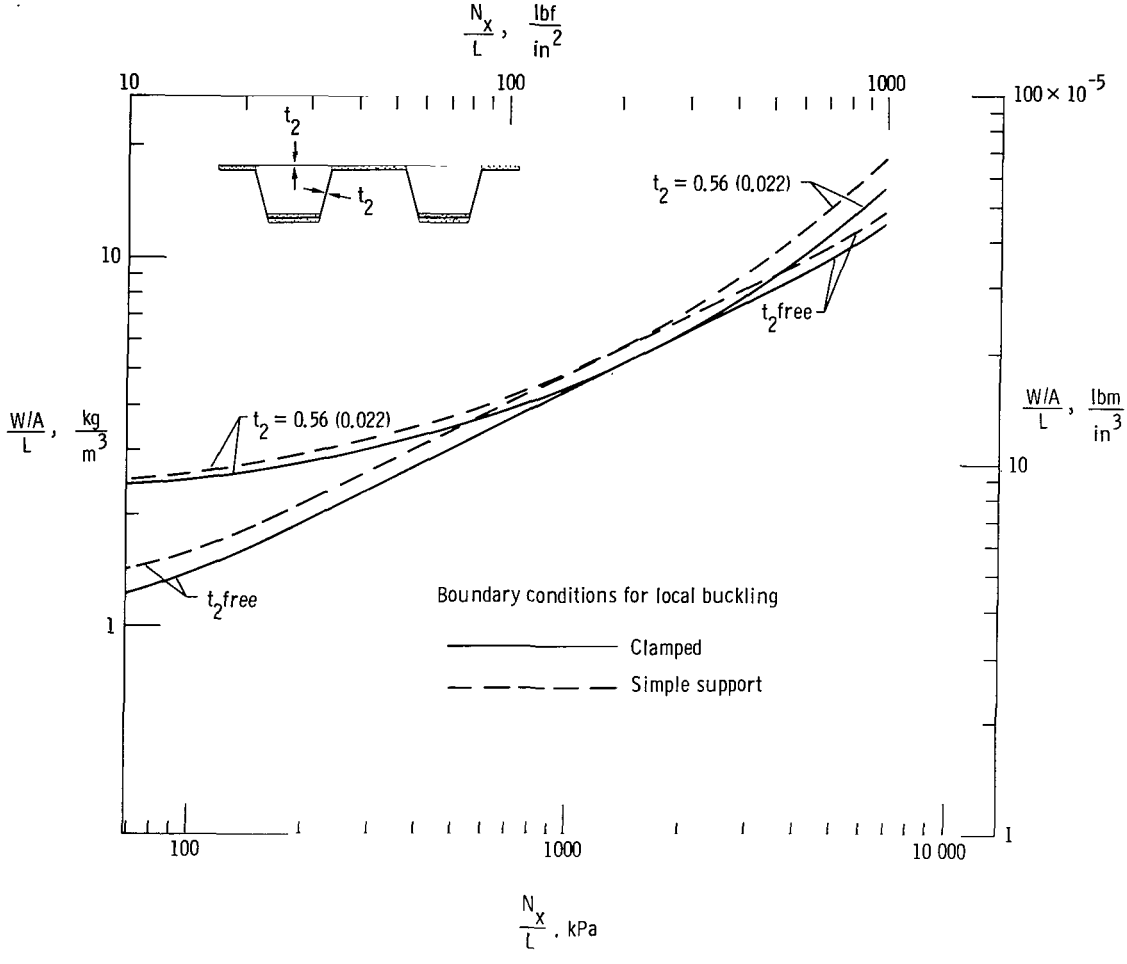

Figure 14.- Effect of local-buckling boundary conditions on structural efficiency of hat-stiffened, graphite-epoxy compression panels; L = 0.76 m (30 in.). Thicknesses are shown in mm (in.).

The benefits derivable from the clamped boundary condition depend upon the curves being compared and the loadings at which the curves are compared. In the loading region where the designs with t_2 = 0.56 mm (0.022 in.) are the most efficient designs, clamping provides a 10-percent reduction in the mass index. These results suggest that a more

sophisticated buckling analysis, such as those described in references 20 and 21, would provide designs that are about 10 percent more efficient than those presented in this report.

Stiffness considerations. - It was shown in reference 5 that the longitudinal extensional stiffness of minimum-mass graphite-epoxy compression panels can be less than that of minimum-mass aluminum panels designed to carry the same load. This fact is demonstrated in figure 15 in which the longitudinal extensional stiffness ET is presented as a function of the loading index $\frac{N_x}{L}$ for a portion of the designs shown in figure 7.

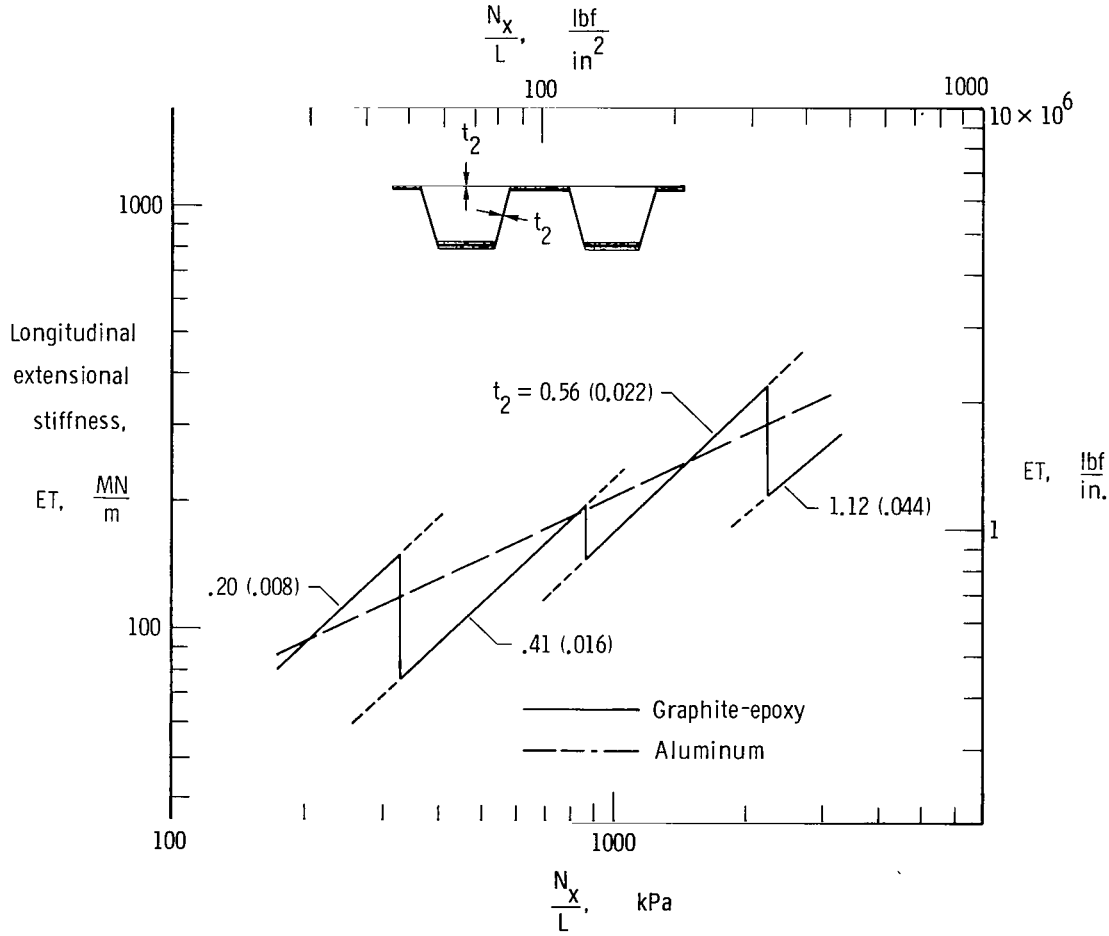

Figure 15. - Longitudinal extensional stiffness as function of loading for minimum-mass, graphite-epoxy and aluminum hat-stiffened compression panels; L = 0.76 m (30 in.). Thicknesses are shown in mm (in.).

The solid lines represent graphite-epoxy panels with four values of t_2, and the dashed line represents aluminum panels. The discontinuities in the extensional stiffness of the

graphite-epoxy designs occur where the most efficient designs shift from one value of t_2 to another. This relationship can be seen by comparing figure 15 with figure 7. The main reason for the "sawtooth" effect in figure 15 is the variation of 0° material in the panels. If stiffness is an important design consideration, that fact can be taken into account by including stiffness constraints in the synthesis procedure.

Aluminum wing panels on commercial jet transports may have a much higher longitudinal extensional stiffness than that shown in figure 15. (See ref. 6.) Commercial aircraft may also have large shear-stiffness requirements as well as stiffener spacing requirements. To study the effect of these additional design requirements, minimum-mass panels were designed for various combinations of extensional and shear stiffness. (Expressions for both stiffnesses are given in the appendix.) All panels were designed to carry a load of $\frac{N_x}{L} = 689$ kPa (100 lbf/in^2), and all panels have a distance d between stiffeners of 12.7 cm (5.0 in.) and a length L of 0.76 m (30 in.). The thickness t_2 is allowed to vary freely.

The results are presented in figure 16 in which the mass index $\frac{W/A}{L}$ of the minimum-mass panels is shown as a function of the design requirements on shear stiffness and longitudinal extensional stiffness. The dashed lines are lines of constant value of the mass index. The circular symbol represents the design which has no stiffness requirement. The solid line above the symbol represents the locus of minimum-mass designs that meet an extensional-stiffness requirement, and the solid line below and to the right of the solid symbol represents the locus of minimum-mass designs that meet a shear-stiffness requirement. Points within the region containing the dashed lines represent designs with combined extensional- and shear-stiffness requirements. The discontinuity in the line defining the extensional-stiffness designs is caused by a change in design concept similar to that shown in figure 12.

Two observations follow from the results presented in figure 16. First, starting at the symbol, increasing either stiffness with a minimum increase in mass (that is, moving along the solid line) causes the other stiffness to decrease. Except for the lower boundary, this characteristic exists for all designs. This characteristic exists primarily because the extensional stiffness is increased by adding 0° material and the shear stiffness is increased with $\pm 45^\circ$ material. Second, the penalty in structural efficiency associated with increasing the shear stiffness is much greater than the penalty associated with increasing the extensional stiffness.

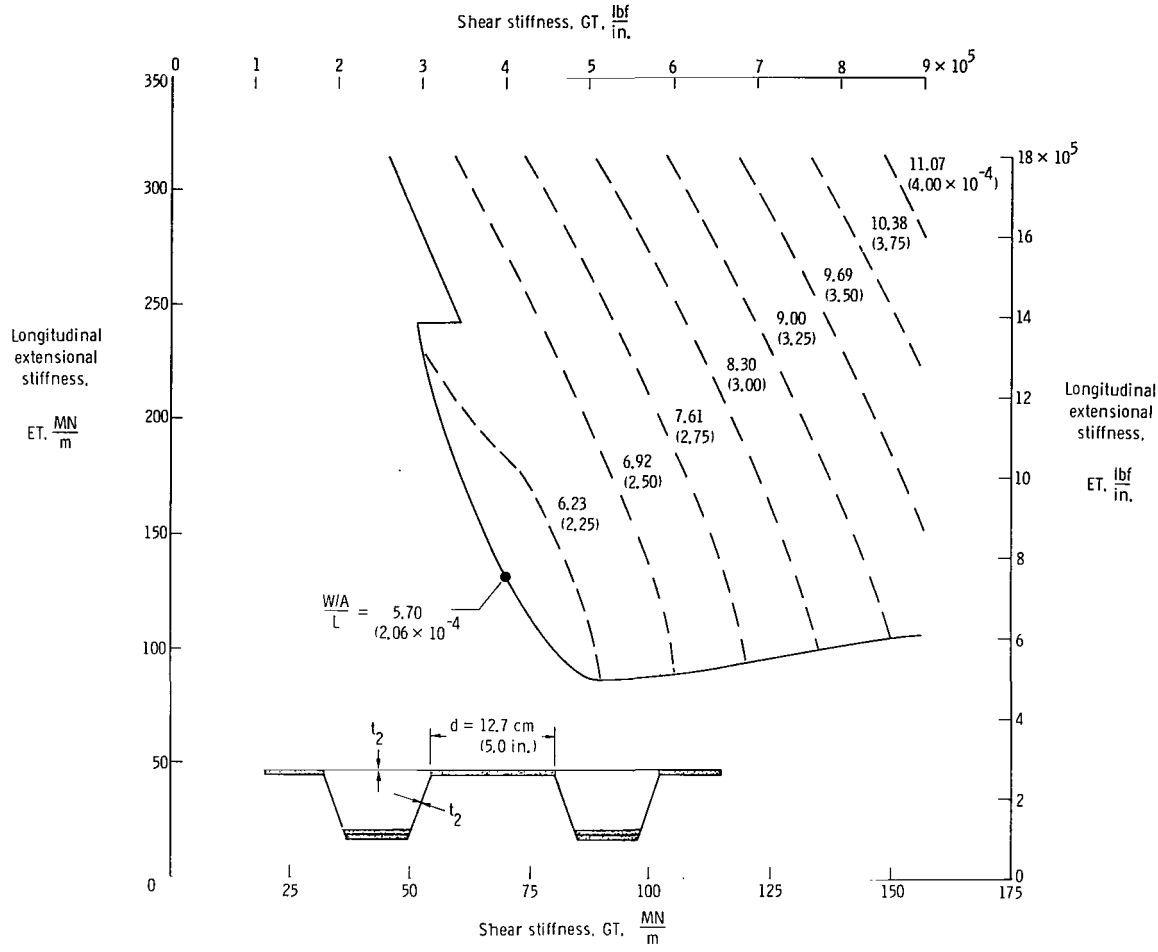

Figure 16.- Panel structural efficiency as function of longitudinal-extensional-stiffness and shear-stiffness requirements for minimum-mass, hat-stiffened, graphite-epoxy compression panels designed to support loading of $\frac{N_x}{L}$ = 689 kPa (100 lbf/in^2). Thickness t_2 varies continuously. Mass index $\frac{W/A}{L}$ given in kg/m^3 (lbm/in^3).

Hat-Stiffened Panel, Combined Shear and Compression

The effect of a shear loading on the structural efficiency of hat-stiffened compression panels is shown in figures 17 and 18. The mass index $\frac{W/A}{L}$ is presented as a function of $\frac{N_x}{L}$ for several values of $\frac{N_{xy}}{L}$ in figure 17 and for several values of $\frac{N_{xy}}{N_x}$ in figure 18. For each curve, t_2 is allowed to vary continuously, so the cusps associated with constant values of t_2 do not appear. As is to be expected, the larger the ratio of $\frac{N_{xy}}{L}$ to $\frac{N_x}{L}$, the larger the effect on the mass index.

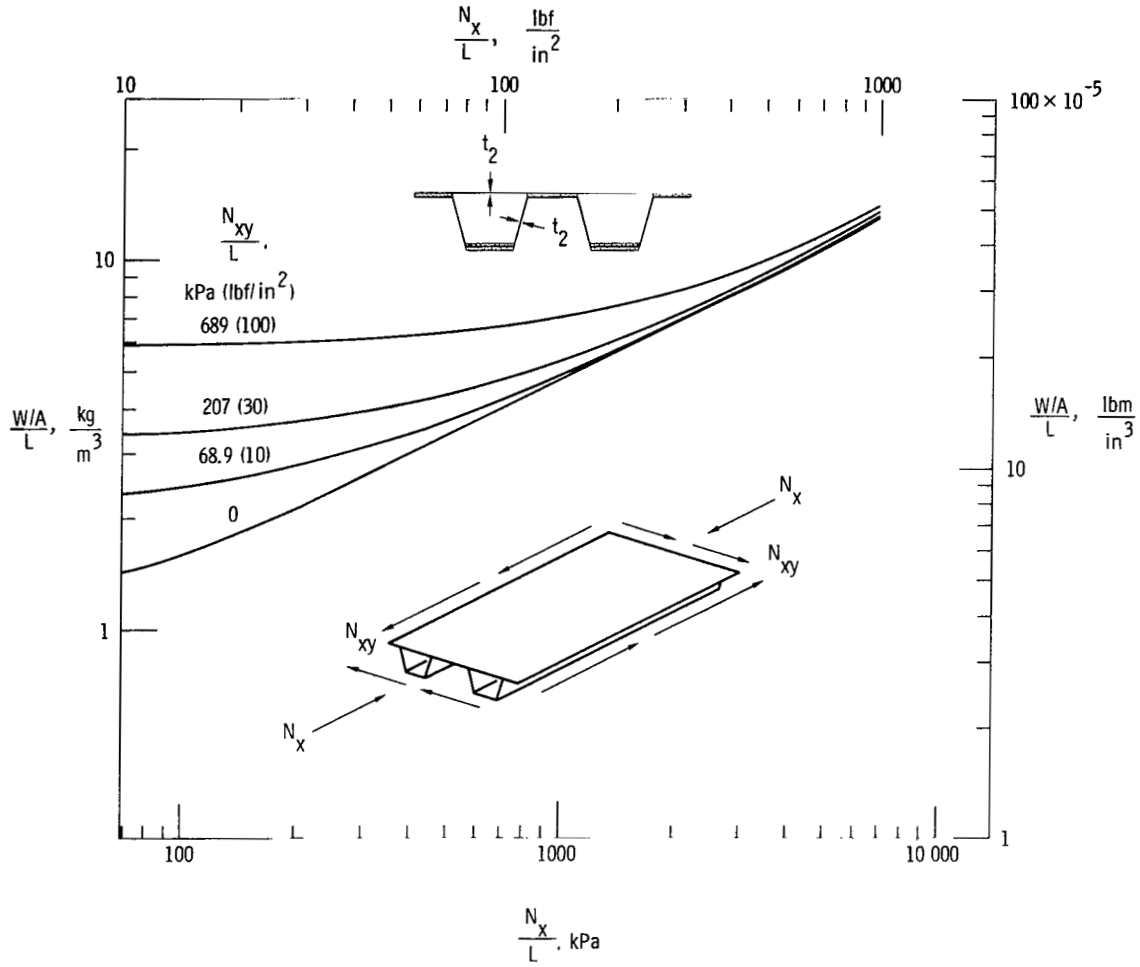

Figure 17.- Effect of shear loading on structural efficiency of hat-stiffened, graphite-epoxy compression panels; L = 0.76 m (30 in.); t_2 varies continuously.

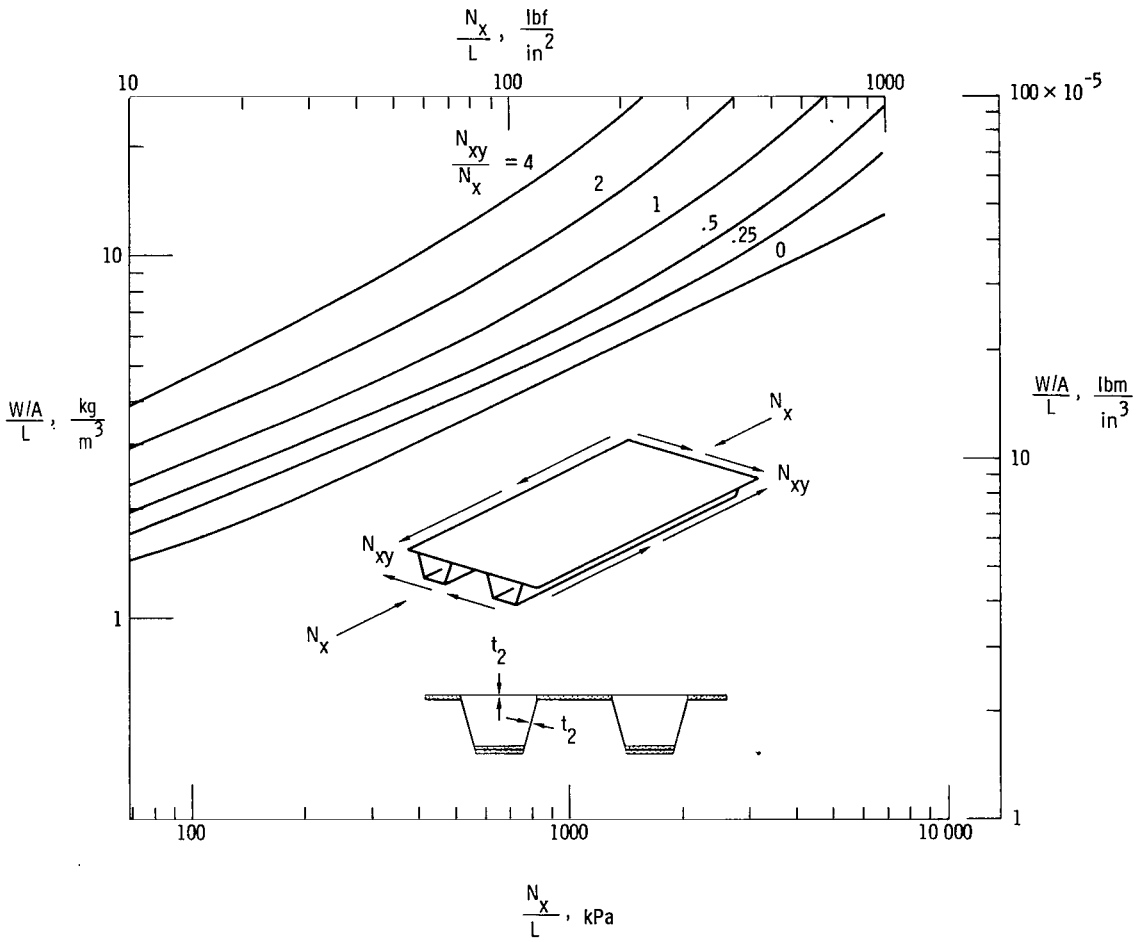

Figure 18.- Structural efficiency of graphite-epoxy, hat-stiffened panels subjected to combinations of longitudinal compression and shear loadings; L = 0.76 m (30 in.); t_2 varies continuously.

Corrugated Panel, Longitudinal Compressive Loading

To study the effect of discrete thickness, corrugated compression panels were designed with various thicknesses of $\pm 45^{o}$ material. The results, which are presented in figure 19, show the same general trends as the hat-stiffened panels (fig. 7). The two main differences are: first, the values of the mass index are lower for the corrugated panel than the hat-stiffened panel; second, the most efficient loading range for a given value of t_2 is lower for a corrugated panel than for a hat-stiffened panel.

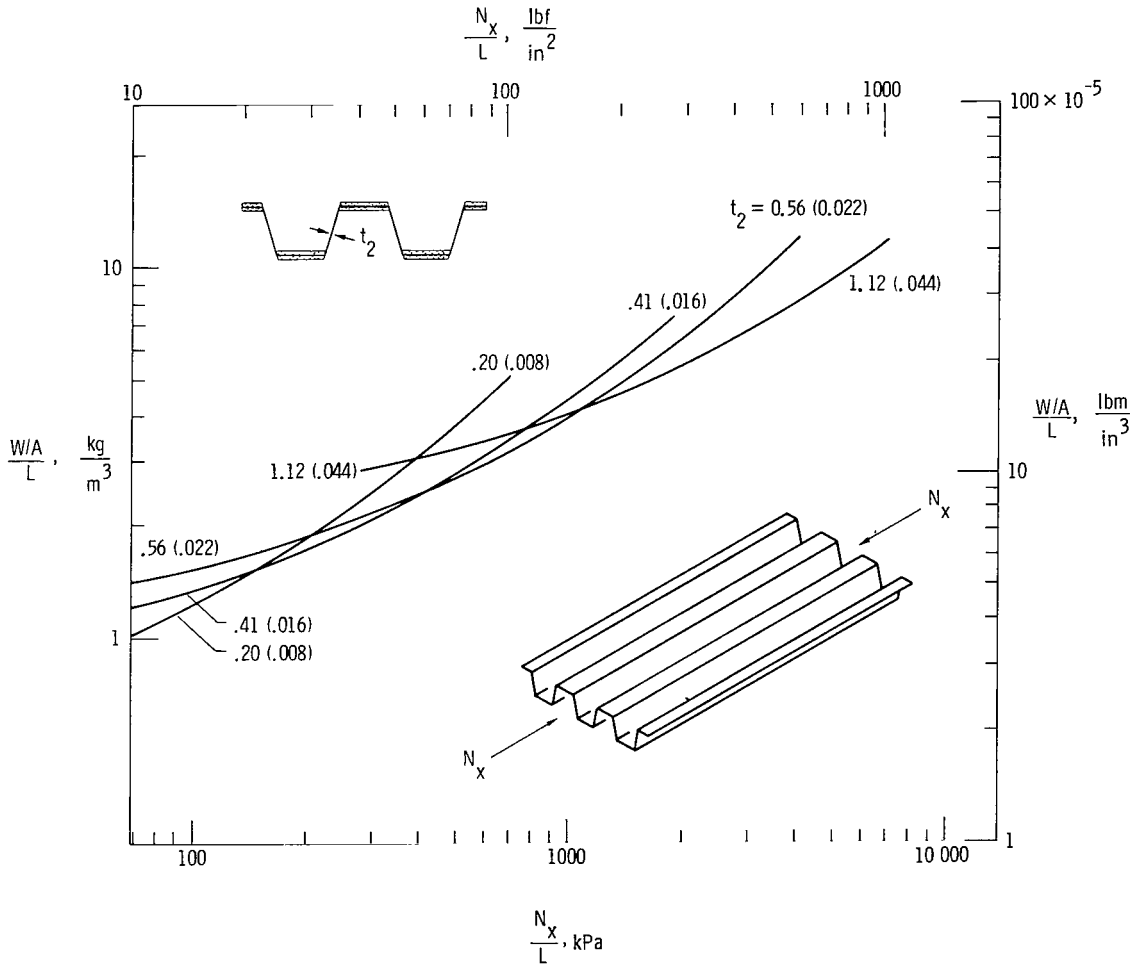

Figure 19.- Structural efficiency of corrugated, graphite-epoxy compression panels for various values of thickness t_2; L = 0.76 m (30 in.). Thicknesses are shown in mm (in.).

Corrugated Panel, Combined Shear and Compression

The effect of a shear loading on the structural efficiency of corrugated compression panels is shown in figures 20 and 21. The curves are similar to those presented in figures 17 and 18. The main difference is that the mass index is lower for the corrugated panels than for the hat-stiffened panels.

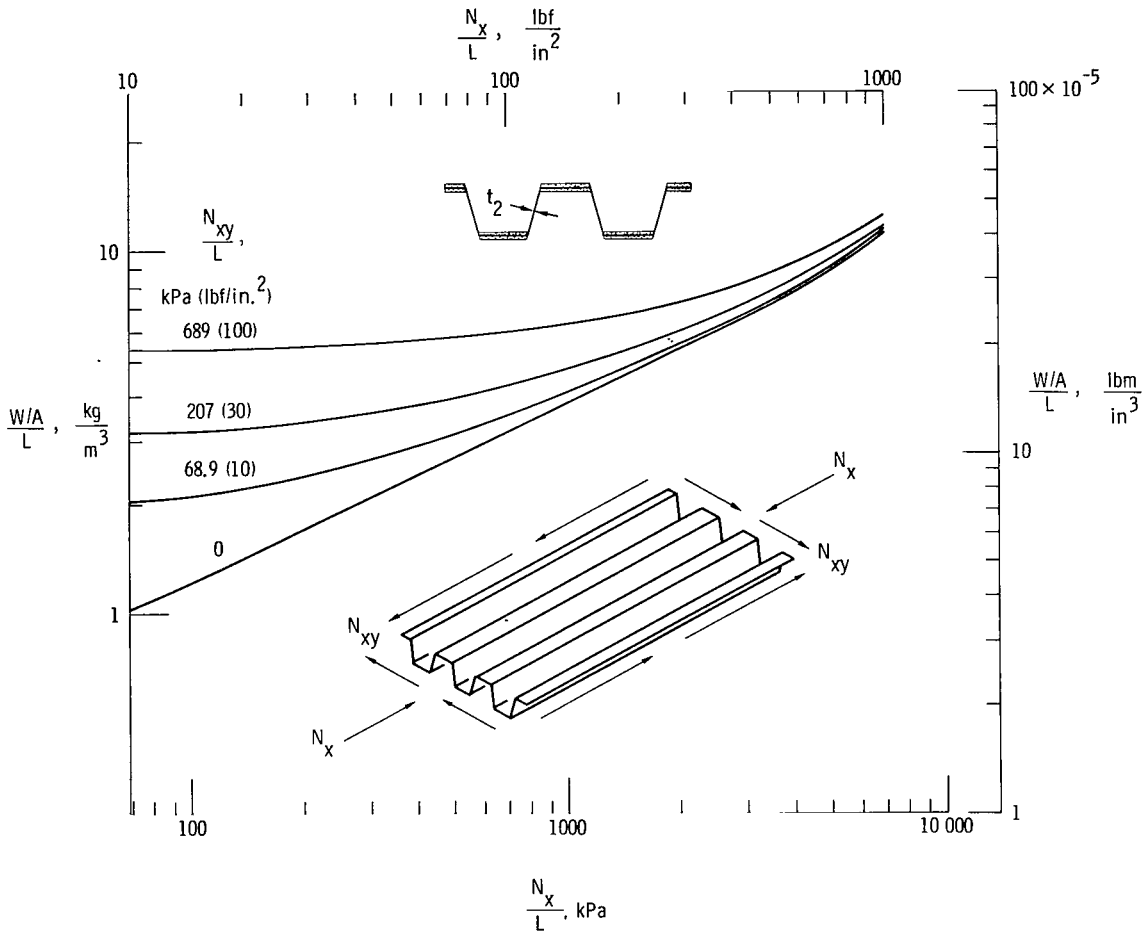

Figure 20.- Effect of shear loading on structural efficiency of corrugated, graphite-epoxy compression panels; L = 0.76 m (30 in.); t_2 varies continuously.

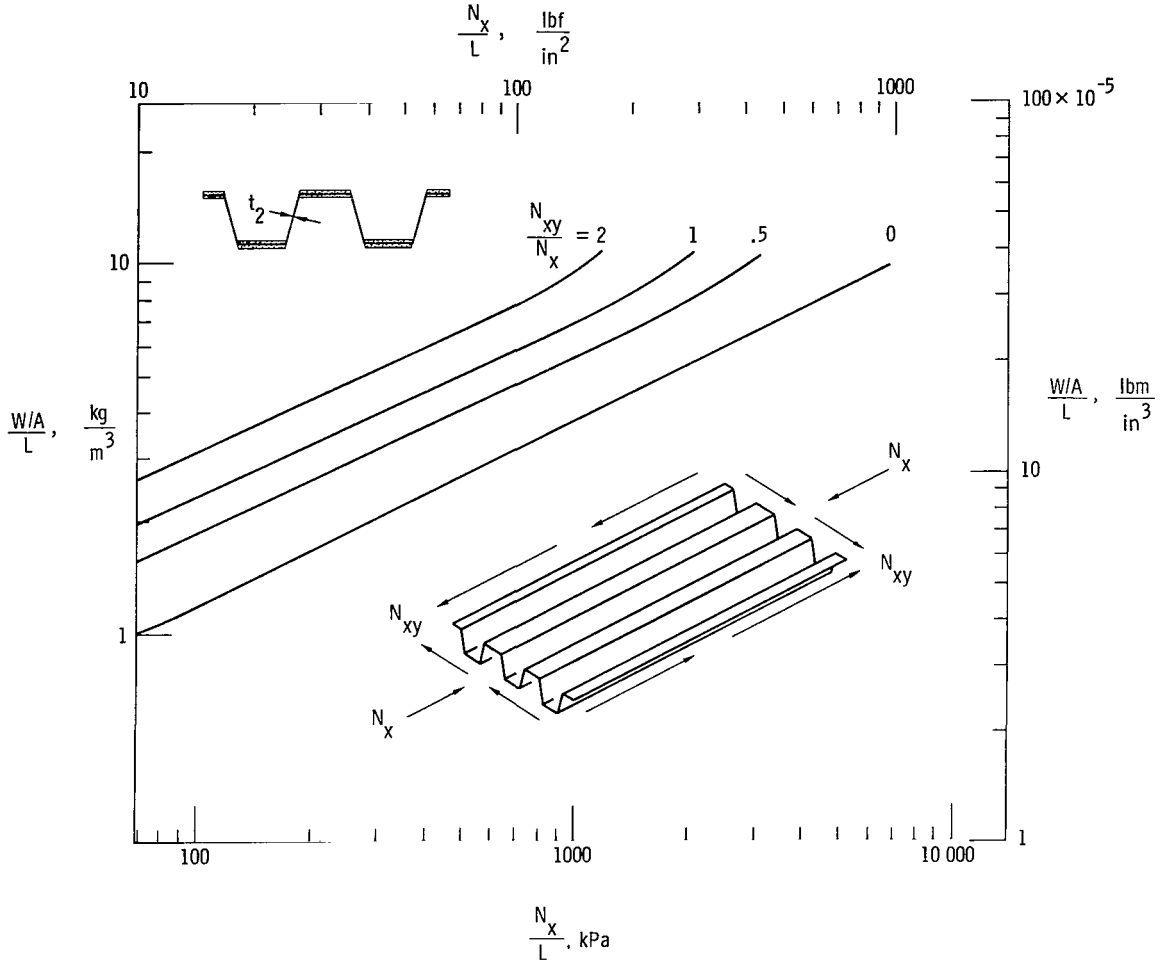

Figure 21.- Structural efficiency of graphite-epoxy corrugated panels subjected to combinations of longitudinal compression and shear loadings; L = 0.76 m (30 in.); t_2 varies continuously.

Hat-Stiffened and Corrugated Panels, Shear Loading

The structural efficiency of hat-stiffened and corrugated panels loaded only by a shear loading is shown in figure 22. The solid curves are for graphite-epoxy panels. Over the range of loading considered, the graphite-epoxy corrugated panels are 5 to 20 percent lighter than the graphite-epoxy hat-stiffened panels.

The dashed curve is for aluminum corrugated panels having uniform thickness and designed using the same procedure as that used for the composite panels. The properties assumed for the aluminum material are given in table V. In the lower loading range $\frac{N_{xy}}{L} < 345$ kPa (50 lbf/in^2), where the panels are buckling critical but not strength critical, the aluminum corrugated panels are about 45 percent heavier than the graphite-epoxy

corrugated panels. For loadings greater than $\frac{N_{xy}}{L}$ = 345 kPa, material strength considerations become dominant for the aluminum panels, and these panels become considerably heavier than the graphite-epoxy panels.

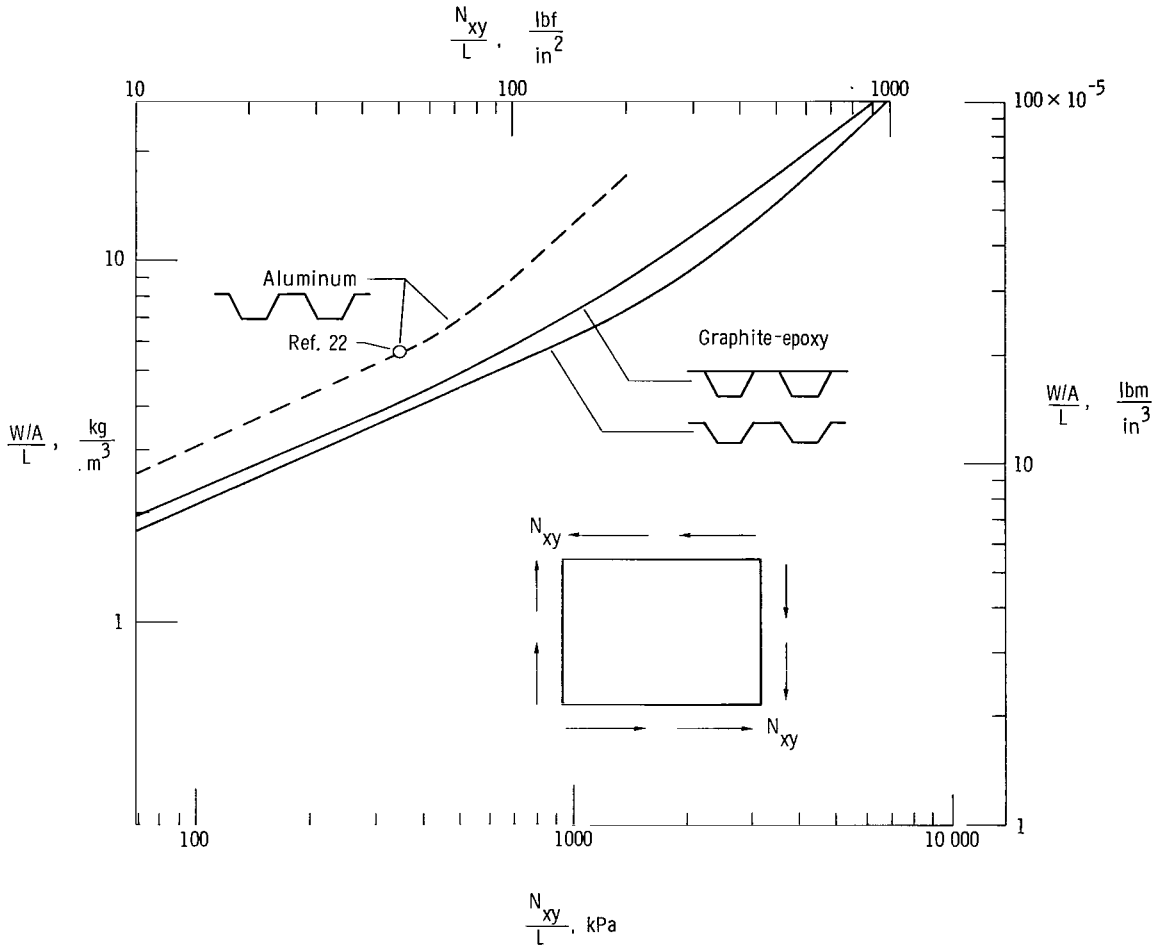

Figure 22.- Effect of shear loading on structural efficiency of graphite-epoxy and aluminum corrugated panels and graphite-epoxy hat-stiffened panels; L = 0.76 m (30 in.); t_2 varies continuously.

The symbol in figure 22 represents the theoretical structural efficiency of an aluminum corrugated shear panel given in reference 22. The structural efficiency of that panel is shown by the intersection of the dashed curves (overall- and local-buckling curves) at $\frac{S}{h^2}$ = 0.05 ksi in figure 9 of reference 22. $\left(\text{The quantity } \frac{S}{h^2} \text{ is the same as } \frac{N_{xy}}{L}.\right)$ The structural efficiency is influenced by a 12-percent increase in mass caused by

doublers at the edges $x = 0$ and $x = L$ and by edge constraints that provide more support than simple-support boundary conditions. That panel is about 3 percent heavier than the aluminum corrugated panel designed with the procedure presented in this report.

CONCLUDING REMARKS

An engineering design procedure for sizing composite hat-stiffened and corrugated panels subjected to longitudinal compression and shear loadings has been developed and exercised. The procedure is based on nonlinear mathematical programing techniques. Expressions are given for the design constraints used in the procedure. These constraints are: overall-buckling loads, local-buckling loads, lamina strength, longitudinal extensional stiffness, and shear stiffness.

The buckling analysis is simplified in that only certain specific buckling modes are considered. Because explicit eigenvalue solutions are available for these buckling modes, eigenvalue analyses are not required. Design studies covering a broad range of design parameters can, therefore, be carried out with a relatively small amount of computer time. Unpublished studies with a more accurate buckling analysis indicate that in most cases the approach is sufficiently accurate to predict structural efficiencies and design trends. In some cases, such as those in which roll modes are active, the buckling analysis approach used here is not adequate.

In order to obtain a clearer understanding of both the analysis-design procedure and the composite panel design results that could be obtained by use of that procedure, several design studies were carried out. Buckling and strength design requirements are included in all the studies. In one study the effect of stiffness requirements is explored. Structural efficiency diagrams are used to present the mass for panels designed to support longitudinal compressive loads, shear loads, and the increase in mass required for combined shear and compressive loadings. The studies indicate that panel mass is not extremely sensitive to panel dimensions; that is, panels with dimensions moderately different from those of the lightest panels may be only slightly heavier than the lightest panels. This fact can be exploited to accommodate manufacturing and other design considerations. It was also determined that scaling techniques in common use for sizing conventional metal panels apply equally well for composite panels where the number of design variables is large.

Other observations, based on limited studies, are:

1. There is a greater mass penalty associated with increasing the shear stiffness of hat-stiffened panels than with increasing the extensional stiffness.

2. The mass of hat-stiffened panels is affected more by changes in the distance between stiffeners than in the width of the hat cap.

3. As has been found in studies for compression panels, composite shear panels offer substantial mass savings over metal shear panels.

The design procedure presented in this report should be used in conjunction with engineering judgment and other analyses to insure the adequacy of the final design. Other design requirements arising from manufacturing considerations, for example, could also have an impact on the design. To the fullest extent possible, all quantifiable requirements should be considered early in the synthesis.

Langley Research Center
National Aeronautics and Space Administration
Hampton, VA 23665
July 23, 1976

APPENDIX

STIFFNESS EXPRESSIONS APPEARING IN ANALYSIS-DESIGN PROCEDURE

Basic Laminate Constitutive Relations

The plate constitutive equation can be written as

$$\left[\begin{array}{c} N_x \\ N_y \\ N_{xy} \\ \hline M_x \\ M_y \\ M_{xy} \end{array}\right] = \left[\begin{array}{ccc:ccc} A_{11} & A_{12} & A_{16} & B_{11} & B_{12} & B_{16} \\ A_{12} & A_{22} & A_{26} & B_{12} & B_{22} & B_{26} \\ A_{16} & A_{26} & A_{66} & B_{16} & B_{26} & B_{66} \\ \hdashline B_{11} & B_{12} & B_{16} & D_{11} & D_{12} & D_{16} \\ B_{12} & B_{22} & B_{26} & D_{12} & D_{22} & D_{26} \\ B_{16} & B_{26} & B_{66} & D_{16} & D_{26} & D_{66} \end{array}\right] \left[\begin{array}{c} \epsilon_x \\ \epsilon_y \\ \gamma_{xy} \\ \hline k_x \\ k_y \\ k_{xy} \end{array}\right] \tag{A1}$$

where A_{ij}, B_{ij}, and D_{ij} are laminate stiffnesses that are calculated from basic material properties by using standard expressions found, for example, in reference 8. The quantities M_x, M_y, and M_{xy} are plate moments, and k_x, k_y, and k_{xy} are the associated curvatures. In all cases considered in this report, the ply-stacking sequence is balanced and symmetric so that the A_{16}, A_{26}, and B_{ij} terms are zero. Also, the D_{16} and D_{26} terms are assumed to be zero. For these types of laminates, which are denoted "specially orthotropic," the set of equations represented by equation (A1) uncouple and reduce to

$$\left[\begin{array}{c} N_x \\ N_y \\ N_{xy} \end{array}\right] = \left[\begin{array}{ccc} A_{11} & A_{12} & 0 \\ A_{12} & A_{22} & 0 \\ 0 & 0 & A_{66} \end{array}\right] \left[\begin{array}{c} \epsilon_x \\ \epsilon_y \\ \gamma_{xy} \end{array}\right] \tag{A2}$$

and

$$\begin{bmatrix} M_x \\ M_y \\ M_{xy} \end{bmatrix} = \begin{bmatrix} D_{11} & D_{12} & 0 \\ D_{12} & D_{22} & 0 \\ 0 & 0 & D_{66} \end{bmatrix} \begin{bmatrix} k_x \\ k_y \\ k_{xy} \end{bmatrix} \tag{A3}$$

In subsequent equations, the notations A_{ij_k} and D_{ij_k} denote the values of A_{ij} and D_{ij}, respectively, for element k.

Extensional Stiffness

If the transverse load N_y is zero, the longitudinal extensional stiffness ET_k of element k is given by

$$ET_k = A_{11_k} - \frac{(A_{12_k})^2}{A_{22_k}} \tag{A4}$$

If it is assumed that all elements of the panel cross section have the same longitudinal strain ϵ_x, the longitudinal extensional stiffness ET is given by

$$ET = \frac{ET_1 b_1 + 2ET_2 b_2 + ET_3 b_3 + 2ET_4 b_4}{b_1 + 2b_4} \tag{A5}$$

For the corrugated panel, ET_1 is zero.

Shear Stiffness

The shear stiffness GT of the panel is defined as

$$GT = \frac{N_{xy}}{\bar{\gamma}_{xy}} \tag{A6}$$

in which $\bar{\gamma}_{xy}$ is the average shear angle given by

$$\bar{\gamma}_{xy} = \frac{2\gamma_{xy_2} b_2 + \gamma_{xy_3} b_3 + 2\gamma_{xy_4} b_4}{b_1 + 2b_4} \tag{A7}$$

With equations (4) to (7) used to calculate the individual shear angles, the shear stiffness GT is

$$GT = \frac{b_1 + 2b_4}{\left(\frac{2b_2}{A_{66_2}} + \frac{b_3}{A_{66_3}}\right)\left(\frac{1}{1 + \frac{2b_2 A_{66_1}}{b_1 A_{66_2}} + \frac{b_3 A_{66_1}}{b_1 A_{66_3}}}\right) + \frac{2b_4}{A_{66_4}}} \tag{A8}$$

Equation (A8) can be used for either hat-stiffened or corrugated panels. For hat-stiffened panels only, the following equation is equivalent to equation (A8) and provides more insight into the effect of the hat on the stiffness GT:

$$GT = \frac{b_1 + 2b_4}{\frac{b_1}{A_{66_1}}\left(1 - \frac{1}{1 + \frac{2b_2A_{66_1}}{b_1A_{66_2}} + \frac{b_3A_{66_1}}{b_1A_{66_3}}}\right) + \frac{2b_4}{A_{66_4}}} \tag{A9}$$

Smeared Stiffnesses for Overall Buckling

The overall-buckling equations given in table III are based on the assumption that the stiffened panel is an orthotropic plate with smeared stiffness properties. The smeared stiffnesses are defined in the following differential equation for lateral deflections of an orthotropic plate loaded as shown in figure 1:

$$\frac{D_x}{1 - \mu_x\mu_y}\frac{\partial^4 w}{\partial x^4} + 2\left(D_{xy} + \frac{\mu_y D_x}{1 - \mu_x\mu_y}\right)\frac{\partial^4 w}{\partial x^2 \partial y^2} + \frac{D_y}{1 - \mu_x\mu_y}\frac{\partial^4 w}{\partial y^4} = -N_x\frac{\partial^2 w}{\partial x^2} + 2N_{xy}\frac{\partial^2 w}{\partial x\,\partial y} \tag{A10}$$

The stiffnesses that appear in equation (A10) are related to the stiffnesses that appear in equations (20) to (23) by

$$D_1 = \frac{D_x}{1 - \mu_x\mu_y} \tag{A11}$$

$$D_2 = \frac{D_y}{1 - \mu_x\mu_y} \tag{A12}$$

$$D_3 = D_{xy} + \frac{\mu_y D_x}{1 - \mu_x\mu_y} \tag{A13}$$

The objective of this section is to provide expressions for EI, D_1, D_2, and D_3. The approach is the same as that used in reference 23.

Calculations presented in reference 23 show that for metal corrugation-stiffened panels, the product $\mu_x\mu_y$ can be neglected when compared with 1.0. It is assumed that the product can also be neglected for composite panels of the type considered in this report.

APPENDIX

Bending stiffnesses EI and D_1.- The panel bending stiffness D_x is simply the EI per unit width of a beam having the cross-sectional shape of the panel. Since $\mu_x\mu_y$ is small compared with 1.0, D_1 is equal to D_x. It is first necessary to locate the neutral axis of the cross section. The distance from the center of element 3 to the neutral axis of element k is denoted z_k. These distances are shown in figure 23 and are summarized below.

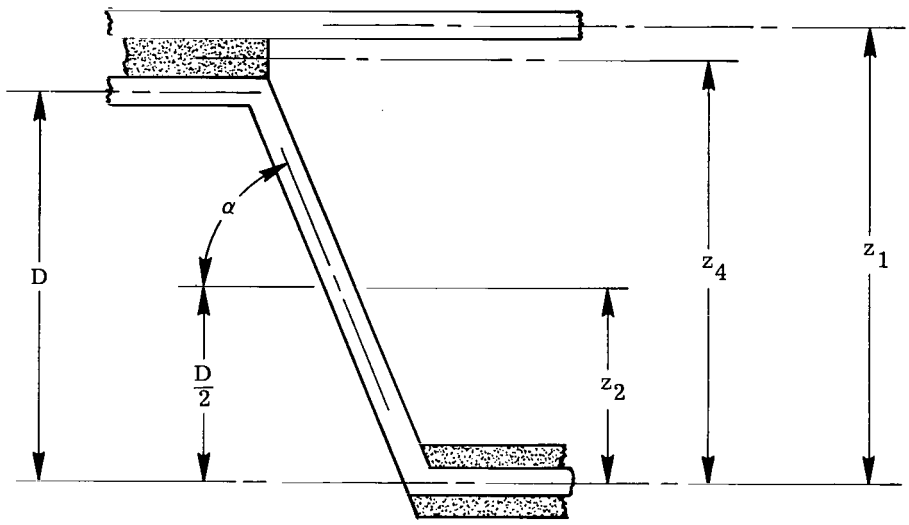

Figure 23.- Additional dimensions for hat-stiffened panel.

	Hat-Stiffened Panel	Corrugated Panel	
z_1	$= D + t_4(0^o) + t_2(\pm 45^o)$	$= D$	(A14)
z_2	$= D/2$	$= D/2$	(A15)
z_3	$= 0$	$= 0$	(A16)
z_4	$= D + \frac{1}{2}\left[t_4(0^o) + t_2(\pm 45^o)\right]$	$= D$	(A17)

The distance z from the center of element 3 to the neutral axis of the panel cross section is then given by

$$\bar{z} = \frac{\sum ET_k b_k z_k}{\sum ET_k b_k} \tag{A18}$$

in which ET_k is given by equation (A4). In equation (A18), proper account must be taken of the fact that elements 2 and 4 appear twice in one period, and the summations are over one period. The bending stiffness EI of one period of the panel cross section is

$$EI = \sum ET_k b_k (z_k - \bar{z})^2 \tag{A19}$$

The bending stiffness of each element about its own centroid is neglected in equation (A19). The error introduced by this assumption is only about 1 percent.

The smeared bending stiffnesses D_x and D_1 are the EI per unit width of the panel

$$D_1 = D_x = \frac{EI}{p} \tag{A20}$$

in which p is the period $b_1 + 2b_4$.

Bending stiffness D_2.- The approach presented in reference 23 is again followed. The smeared bending stiffness in the y-direction is given by

$$D_y = D_2 = \frac{p}{\dfrac{2b_4}{D_{22_4}} + \dfrac{b_1}{\dfrac{b_1}{2X} + D_{22_1}}} \tag{A21}$$

where

$$X = \frac{b_2}{D_{22_2}} + \frac{b_3}{2D_{22_3}} - H\left(\frac{b_2^2 \sin\alpha}{2D_{22_2}} + \frac{Db_3}{2D_{22_3}}\right) \tag{A22}$$

and

$$H = \frac{\dfrac{b_2^2}{2}\dfrac{\sin\alpha}{D_{22_2}} + \dfrac{b_3}{2}\dfrac{D}{D_{22_3}}}{\dfrac{b_2^3}{3}\dfrac{\sin^2\alpha}{D_{22_2}} + \dfrac{b_3}{2}\dfrac{D^2}{D_{22_3}}} \tag{A23}$$

Angle α is the angle that element 2 makes with the horizontal as shown in figure 23.

Stiffness D_3.- For the hat-stiffened panel, $\mu_y D_x$ can be neglected when compared with D_{xy}. In this case $D_3 = D_{xy}$. The twisting stiffness D_{xy} is calculated from Bredt theory (see, for example, ref. 24) and is given by

$$D_3 = D_{xy} = \frac{2\overline{A}^2}{p\left(\frac{b_1}{A66_1} + \frac{2b_2}{A66_2} + \frac{b_3}{A66_3}\right)} \tag{A24}$$

in which $\overline{A}$ is the area enclosed by the hat and is given by

$$\overline{A} = \frac{1}{2}(b_1 + b_3)\left[D + t_4(0^o) + t_2(\pm 45^o)\right] \tag{A25}$$

Experimental work presented in reference 23 and analytical studies carried out to support reference 25 indicate that the value of D_{xy} given in equation (A24) is too large. In the studies presented in this report the twisting stiffness was obtained by applying a 0.3 factor to the value given by equation (A24).

In the case of the corrugated panel, $\mu_y D_x$ cannot be ignored when compared with D_{xy}. The stiffness D_3 is given by

$$D_3 = \frac{2b_2\left(D12_2 + 2D66_2\right) + 2b_3\left(D12_3 + 2D66_3\right)}{p} \tag{A26}$$

REFERENCES

1. Waddoups, M. E.; McCullers, L. A.; Olson, F. O.; and Ashton, J. E.: Structural Synthesis of Anisotropic Plates. Paper presented at AIAA/ASME 11th Structures, Structural Dynamics, and Materials Conference (Denver, Colorado), Apr. 1970.

2. Peterson, James P.: Structural Efficiency of Aluminum Multiweb Beams and Z-Stiffened Panels Reinforced With Filamentary Boron-Epoxy Composite. NASA TN D-5856, 1970.

3. Agarwal, Banarsi; and Davis, Randall C.: Minimum-Weight Designs for Hat-Stiffened Composite Panels Under Uniaxial Compression. NASA TN D-7779, 1974.

4. McCullers, L. A.: Automated Design of Advanced Composite Structures. Structural Optimization Symposium, L. A. Schmit, Jr., ed., AMD-Vol. 7, Amer. Soc. Mech. Eng., Nov. 1974, pp. 119-133.

5. Williams, Jerry G.; and Mikulas, Martin M., Jr.: Analytical and Experimental Study of Structurally Efficient Composite Hat-Stiffened Panels Loaded in Axial Compression. AIAA Paper No. 75-754, May 1975.

6. Mikulas, Martin M., Jr.; Bush, Harold G.; and Rhodes, Marvin D.: Current Langley Research Center Studies on Buckling and Low-Velocity Impact of Composite Panels. Third Conference on Fibrous Composites in Flight Vehicle Design, Part II, NASA TM X-3377, 1976.

7. Ashton, J. E.; Halpin, J. C.; and Petit, P. H.: Primer on Composite Materials: Analysis. Technomic Pub. Co., Inc., c.1969.

8. Advanced Composites Design Guide. Volumes I-V. Third ed., U.S. Air Force, Jan. 1973.

9. Schmit, Lucien A., Jr.; Kicher, Thomas P.; and Morrow, William M.: Structural Synthesis Capability for Integrally Stiffened Waffle Plates. AIAA J., vol. 1, no. 12, Dec. 1963, pp. 2820-2836.

10. Morrow, William M., II; and Schmit, Lucien A., Jr.: Structural Synthesis of a Stiffened Cylinder. NASA CR-1217, 1968.

11. Timoshenko, S.: Theory of Elastic Stability. McGraw-Hill Book Co., Inc., 1936.

12. Stein, Manuel; and Mayers, J.: Compressive Buckling of Simply Supported Curved Plates and Cylinders of Sandwich Construction. NACA TN 2601, 1952.

13. Lekhnitskii, S. G. (S. W. Tsai and T. Cheron, transl.): Anisotropic Plates. Gordon & Breach Sci. Publ., Inc., c.1968.

14. Batdorf, S. B.; and Stein, Manuel: Critical Combinations of Shear and Direct Stress for Simply Supported Rectangular Flat Plates. NACA TN 1223, 1947.

15. Housner, Jerrold M.; and Stein, Manuel: Numerical Analysis and Parametric Studies of the Buckling of Composite Orthotropic Compression and Shear Panels. NASA TN D-7996, 1975.

16. Hague, Donald S.; and Glatt, Curtis R.: An Introduction to Multivariable Search Techniques for Parameter Optimization (and Program AESOP). Contract No. NAS 2-4507, Boeing Co., Apr. 1968. (Available as NASA CR-73200.)

17. Hague, D. S.; and Glatt, C. R.: A Guide to the Automated Engineering and Scientific Optimization Program, AESOP. Contract NAS 2-4507, Space Div., Boeing Co., [1968]. (Available as NASA CR-73201.)

18. Jones, R. T.; and Hague, D. S.: Application of Multivariable Search Techniques to Structural Design Optimization. NASA CR-2038, 1972.

19. Shanley, F. R.: Weight-Strength Analysis of Aircraft Structures. Second ed., Dover Publ., Inc., c.1960.

20. Viswanathan, A. V.; and Tamekuni, M.: Elastic Buckling Analysis for Composite Stiffened Panels and Other Structures Subjected to Biaxial Inplane Loads. NASA CR-2216, 1973.

21. Wittrick, W. H.; and Williams, F. W.: Buckling and Vibration of Anisotropic or Isotropic Plate Assemblies Under Combined Loadings. Int. J. Mech. Sci., vol. 16, no. 4, Apr. 1974, pp. 209-239.

22. Peterson, James P.; and Card, Michael F.: Investigation of the Buckling Strength of Corrugated Webs in Shear. NASA TN D-424, 1960.

23. Stroud, W. Jefferson: Elastic Constants for Bending and Twisting of Corrugation-Stiffened Panels. NASA TR R-166, 1963.

24. Kuhn, Paul: Stresses in Aircraft and Shell Structures. McGraw-Hill Book Co., Inc., 1956.

25. Agarwal, B. L.; and Sobel, L. H.: Weight Comparisons of Optimized Stiffened, Unstiffened, and Sandwich Cylindrical Shells Made From Composite or Aluminum Materials. Proceedings AIAA/ASME/SAE 17th Structures, Structural Dynamics, and Materials Conference, King of Prussia, Pa., May 5-7, 1976, pp. 333-343.

TABLE I.- EQUATIONS FOR STRESS ANALYSIS

Loading-equation identification	Equation	Equation number
Longitudinal compression	$\epsilon_x = \frac{N_x}{ET}$	(1)
	$\epsilon_{y_k} = -\epsilon_x \frac{A_{12_k}}{A_{22_k}}$	(2)
	$N_{x_k} = \epsilon_x E T_k$	(3)
Shear	$N_{xy_4} = N_{xy}$	(4)
	$N_{xy_2} = N_{xy_3} = \frac{N_{xy}}{1 + \frac{2b_2}{b_1}\frac{A_{66_1}}{A_{66_2}} + \frac{b_3}{b_1}\frac{A_{66_1}}{A_{66_3}}}$	(5)
	$N_{xy_1} = N_{xy} - N_{xy_2}$	(6)
	$\gamma_{xy_k} = \frac{N_{xy_k}}{A_{66_k}}$	(7)
Lamina strains referred to lamina principal axes	$\epsilon_1 = \cos^2\theta\,\epsilon_x + \sin^2\theta\,\epsilon_y + \cos\theta\sin\theta\,\gamma_{xy}$	(8)
	$\epsilon_2 = \sin^2\theta\,\epsilon_x + \cos^2\theta\,\epsilon_y - \cos\theta\sin\theta\,\gamma_{xy}$	(9)
	$\gamma_{12} = -2\sin\theta\cos\theta\,\epsilon_x + 2\sin\theta\cos\theta\,\epsilon_y + \left(\cos^2\theta - \sin^2\theta\right)\gamma_{xy}$	(10)
Lamina stresses referred to lamina principal axes	$\sigma_1 = Q_{11}\epsilon_1 + Q_{12}\epsilon_2$	(11)
	$\sigma_2 = Q_{12}\epsilon_1 + Q_{22}\epsilon_2$	(12)
	$\tau_{12} = Q_{66}\gamma_{12}$	(13)

TABLE II.- EQUATIONS FOR STRENGTH FAILURE CRITERIA

Failure criterion	Equation (*)	Equation number
Maximum strain	$\frac{\epsilon_1}{\epsilon_1^a} \leqq 1$	(14)
	$\frac{\epsilon_2}{\epsilon_2^a} \leqq 1$	(15)
	$\frac{\gamma_{12}}{\gamma_{12}^a} \leqq 1$	(16)
Stress interaction	$\frac{\sigma_1}{\sigma_1^a} \leqq 1$	(17)
	$\left(\frac{\sigma_2}{\sigma_2^a}\right)^2 + \left(\frac{\tau_{12}}{\tau_{12}^a}\right)^2 \leqq 1$	(18)

*Superscript a denotes allowable value.

TABLE III.- EQUATIONS FOR OVERALL AND LOCAL BUCKLING

Loading	Equation	Equation number	References
	Overall buckling		
Longitudinal compression	$N_{x,crit} = \frac{\pi^2 EI}{pL^2} \frac{1}{1 + \frac{\pi^2 EI}{2L^2 b_2 A_{66_2}}}$	(19)	Equation (92'), ref. 11; equation (3), ref. 12
Shear	$\theta = \frac{\sqrt{D_1 D_2}}{D_3}$	(20)	Equations (2.2.2-21) and (2.2.2-22), ref. 8; see, also pp. 383-384, ref. 11; pp. 468-471, ref. 13
	For $\theta > 1$, $N_{xy,crit} = \left(\frac{2}{L}\right)^2 \left(D_1^3 D_2\right)^{1/4} \left(8.125 + \frac{5.05}{\theta}\right)$	(21)	
	For $\theta < 1$, $N_{xy,crit} = \left(\frac{2}{L}\right)^2 \left(D_1 D_3\right)^{1/2} \left(11.7 + 0.532\theta + 0.938\theta^2\right)$	(22)	
Combined loads	Loading critical when $\frac{N_x}{N_{x,crit}} + \left(\frac{N_{xy}}{N_{xy,crit}}\right)^2 = 1$	(23)	Equation (105.8), ref. 13; refs. 14 and 15
	Local buckling; equations applied to each element		
Longitudinal compression	$N_{x,crit} = \frac{2\pi^2}{b^2} \left[\left(D_{11} D_{22}\right)^{1/2} + D_{12} + 2D_{66}\right]$	(24)	Equation (2.2.2-16), ref. 8; equation (233), ref. 11
Shear	$\theta = \frac{\left(D_{11} D_{22}\right)^{1/2}}{D_{12} + 2D_{66}}$	(25)	Equations (2.2.2-21) and (2.2.2-22), ref. 8; see, also pp. 383-384, ref. 11; pp. 468-471, ref. 13
	For $\theta > 1$, $N_{xy,crit} = \left(\frac{2}{b}\right)^2 \left(D_{11} D_{22}^3\right)^{1/4} \left(8.125 + \frac{5.05}{\theta}\right)$	(26)	
	For $\theta < 1$, $N_{xy,crit} = \left(\frac{2}{b}\right)^2 \left[D_{22}\left(D_{12} + 2D_{66}\right)\right]^{1/2} \left(11.7 + 0.532\theta + 0.938\theta^2\right)$	(27)	
Combined loads	Loading critical when $\frac{N_x}{N_{x,crit}} + \left(\frac{N_{xy}}{N_{xy,crit}}\right)^2 = 1$	(28)	Equation (105.8), ref. 13; ref. 15

TABLE IV.- PROPERTIES OF GRAPHITE-EPOXY MATERIAL USED IN SAMPLE CALCULATIONS

[ten. denotes tension; comp. denotes compression; and superscript a indicates allowable]

Symbol	Value in SI units	Value in U.S. Customary units
Density and elastic properties		
ρ	1520 kg/m^3	0.055 lbm/in^3
E_1	145 GPa	21×10^6 psi
E_2	16.5 GPa	2.39×10^6 psi
G_{12}	4.48 GPa	0.65×10^6 psi
μ_{12}	0.314	0.314
μ_{21}	0.037	0.037
Allowable stresses		
σ_1^a (ten.)	1240 MPa	180 ksi
σ_1^a (comp.)	-1240 MPa	-180 ksi
σ_2^a (ten.)	55.2 MPa	8 ksi
σ_2^a (comp.)	-207 MPa	-30 ksi
τ_{12}^a	82.7 MPa	12 ksi
Allowable strains		
ϵ_1^a (ten.)	0.0087	0.0087
ϵ_1^a (comp.)	-0.0087	-0.0087
ϵ_2^a (ten.)	0.00475	0.00475
ϵ_2^a (comp.)	-0.01764	-0.01764
γ_{12}^a	0.01846	0.01846

TABLE V.- PROPERTIES OF ALUMINUM USED IN SAMPLE CALCULATIONS

Material properties		
Symbol	Value in SI units	Value in U.S. Customary units
ρ	2780 kg/m^3	0.101 lbm/in^3
E	72.4 GPa	10.5×10^6 psi
G	27.4 GPa	3.98×10^6 psi
μ	0.32	0.32
τ_a	221 MPa	32 ksi

TABLE VI.- LIMITS ON DESIGN VARIABLES

Dimension	Hat-stiffened panel		Corrugated panel	
	cm	in.	cm	in.
$t_3(0^o)$, maximum	0.318	0.125	0.318	0.125
$t_4(0^o)$, maximum	.635	.250	Not applicable	
b_1, minimum	2.03	.80	2.03	.80
b_2, minimum	1.02	.40	1.02	.40
b_3, minimum	2.03	.80	2.03	.80
b_4, minimum	1.02	.40	Not applicable	

"The aeronautical and space activities of the United States shall be conducted so as to contribute . . . to the expansion of human knowledge of phenomena in the atmosphere and space. The Administration shall provide for the widest practicable and appropriate dissemination of information concerning its activities and the results thereof."

—NATIONAL AERONAUTICS AND SPACE ACT OF 1958

NASA SCIENTIFIC AND TECHNICAL PUBLICATIONS

TECHNICAL REPORTS: Scientific and technical information considered important, complete, and a lasting contribution to existing knowledge.

TECHNICAL NOTES: Information less broad in scope but nevertheless of importance as a contribution to existing knowledge.

TECHNICAL MEMORANDUMS: Information receiving limited distribution because of preliminary data, security classification, or other reasons. Also includes conference proceedings with either limited or unlimited distribution.

CONTRACTOR REPORTS: Scientific and technical information generated under a NASA contract or grant and considered an important contribution to existing knowledge.

TECHNICAL TRANSLATIONS: Information published in a foreign language considered to merit NASA distribution in English.

SPECIAL PUBLICATIONS: Information derived from or of value to NASA activities. Publications include final reports of major projects, monographs, data compilations, handbooks, sourcebooks, and special bibliographies.

TECHNOLOGY UTILIZATION PUBLICATIONS: Information on technology used by NASA that may be of particular interest in commercial and other non-aerospace applications. Publications include Tech Briefs, Technology Utilization Reports and Technology Surveys.

Details on the availability of these publications may be obtained from:

SCIENTIFIC AND TECHNICAL INFORMATION OFFICE

NATIONAL AERONAUTICS AND SPACE ADMINISTRATION

Washington, D.C. 20546